

Exploring the Properties of the Phases of QCD Matter

Research opportunities and priorities for the next decade

Summary of the “Phases of QCD Matter” Town Meeting
at Temple University, Philadelphia, 13-15 Sep. 2014

Prepared for consideration in the
2015 NSAC Long Range Plan for Nuclear Physics

Ulrich Heinz (Ohio State University) and Paul Sorensen (BNL), co-conveners;
Carl Gagliardi (Texas A&M University),
Frithjof Karsch (BNL & Universität Bielefeld),
Tuomas Lappi (University of Jyväskylä),
Berndt Müller (BNL & Duke University),
Jamie Nagle (University of Colorado),
Krishna Rajagopal (MIT),
Gunther Roland (MIT),
Raju Venugopalan (BNL).

January 4, 2015

Abstract

This document provides a summary of the discussions during the recent joint QCD Town Meeting at Temple University of the status of and future plans for the research program of the relativistic heavy-ion community. A list of recommendations outlining the greatest research opportunities and detailing the research priorities of the heavy-ion community, voted on and unanimously approved at the Town Meeting, is presented. They are supported by a broad discussion of the underlying physics and its relation to other subfields. Areas of overlapping interests with the “QCD and Hadron Structure” (“cold QCD”) subcommunity, in particular the recommendation for the future construction of an Electron-Ion Collider, are emphasized. The agenda of activities of the “hot QCD” subcommunity at the Town Meeting is attached.

Contents

1	Executive Summary	3
2	Overview and Recommendations	5
2.1	Where we stand: recent insights and open questions	5
2.2	Accomplishments and future goals	6
2.3	Recommendations	8
2.3.1	New questions and opportunities in relativistic heavy-ion collisions	8
2.3.2	A precision femtoscope to study the glue that binds us all	10
2.3.3	New initiatives to further strengthen nuclear theory	10
2.3.4	Educating and mentoring the next generation of scientists	11
3	Quantifying the Properties of QCD Matter - Now and Tomorrow	12
3.1	Completing the Little Bang Standard Model	12
3.2	Mapping the QCD phase diagram	16
3.3	Probing hot QCD matter at multiple length scales	21
3.3.1	Jets as microscopic probes of QGP	21
3.3.2	Probing the QGP with bottomonia	26
3.4	A polarized p+A program for initial-state and low-x phenomena	26
3.5	Opportunities and challenges in theory	28
3.5.1	Progress since the 2007 Nuclear Physics Long Range Plan	28
3.5.2	Open questions and future goals	29
3.5.3	What the field needs	31
4	The Electron Ion Collider	33
4.1	The next QCD frontier	33
4.2	Science highlights and deliverables at the EIC	34
4.3	EIC machine parameters and designs	37
4.4	Why now?	37
5	Bibliography	38
6	Appendix: Town Meeting Agenda	48

1 Executive Summary

On September 13-15, 2014, the QCD Community within the APS Division of Nuclear Physics met at Temple University, Philadelphia, for a three-day Town Meeting to discuss the status and future priorities of their research program, in preparation for a new Long Range Plan for Nuclear Physics to be written and submitted to the NSF and DOE Nuclear Science Advisory Committee in 2015. The U.S. Nuclear Physics QCD Community consists of two, partially overlapping, subcommunities whose activities focus on “The Phases of QCD Matter” (a.k.a. as “hot QCD community”) and “QCD and Hadron Structure” (a.k.a. as “cold QCD community”), respectively. Their joint Town Meeting featured a daylong *joint session* (spread over two days, from 4pm on Saturday to 4 pm on Sunday), with *separate sessions* of the “hot” and “cold” QCD subcommunities scheduled in parallel for the rest of the time. The Town Meeting program schedule, including links to the slides of all presentations, can be found at <https://indico.bnl.gov/conferenceDisplay.py?confId=857>. With 244 registrants (108 from “hot QCD”, 136 from “cold QCD”), participation by the community in the 2014 joint QCD Town Meeting was about 10% stronger than for the corresponding meeting in early 2007 at Rutgers University, reflecting the health and strength of the U.S. QCD Community in Nuclear Physics. Strong community interest in the planning for the next decade was also reflected in a total of 49 short presentations submitted and delivered by participants, in addition to the 47 invited talks (15 and 19 in the “hot” and “cold” QCD parallel sessions, respectively, and 13 in the joint session) that were solicited, with detailed charges to the speakers to ensure a well-rounded program, by the Town Meeting conveners (Haiyan Gao, Ulrich Heinz, Craig Roberts, and Paul Sorensen).

This document summarizes those parts of the Town Meeting activities in which the “hot QCD” community played a key role (i.e. the joint session and the “hot QCD” parallel sessions). A similar but separate document by the “cold QCD” community complements it with a summary of their activities at the joint QCD Town Meeting. In this Executive Summary we list the recommendations that were voted on and unanimously approved during the joint session and the separate “hot QCD” parallel voting session. Recommendation #2 on the construction of an Electron Ion Collider was discussed and unanimously approved during the joint session, as the *highest priority for future new construction* (after the completion of FRIB) of the entire U.S. QCD Community in Nuclear Physics. Recommendation #4 was passed unanimously in identical form by both subcommunities in their parallel voting sessions. Recommendation #3 is an amended version of a recommendation passed by overwhelming majority in the joint session to “endorse the new initiatives and investments proposed in the Recommendation and Request received from the Computational Nuclear Physics Town Meeting.” The amended version listed here was passed unanimously in a later vote taken during the separate voting session of the “hot QCD” community. Recommendation #1 represents the highest priority for the future of the ongoing research program of the “Phases of QCD Matter” community; it also passed unanimously during the “hot QCD” voting session. Here are the four recommendations:

- **Recommendation #1:**

The discoveries of the past decade have posed or sharpened questions that are central to understanding the nature, structure, and origin of the hottest liquid form of matter that the universe has ever seen. As our highest priority we recommend a program to complete the search for the critical point in the QCD phase diagram and to exploit the newly realized potential of exploring the QGP’s structure at multiple length scales with jets at RHIC and LHC energies. This requires

- **implementation of new capabilities of the RHIC facility (a state-of-the-art jet detector such as sPHENIX and luminosity upgrades for running at low energies) needed to**

46 **complete its scientific mission,**

47 – **continued strong U.S. participation in the LHC heavy-ion program, and**

48 – **strong investment in a broad range of theoretical efforts employing various analytical**
49 **and computational methods.**

50 • **Recommendation #2:**

51 **A high luminosity, high-energy polarized Electron Ion Collider (EIC) is the U.S. QCD**
52 **community’s highest priority for future construction.**

53 • **Recommendation #3:**

54 **We endorse the new initiatives and investments proposed in the Recommendation and**
55 **Request received from the Computational Nuclear Physics Town Meeting, at a level to**
56 **be determined by the requested NSAC subcommittee. In addition, we recommend new**
57 **funding to expand the successful “Topical Collaborations in Nuclear Theory” program**
58 **initiated in the last Long Range Plan of 2007, to a level of at least one new Topical**
59 **Collaboration per year.**

60 • **Recommendation #4:**

61 **The QCD community endorses and supports the conclusions from the Education and**
62 **Innovation Town Meeting.**

63 The rest of this document provides supporting arguments for these recommendations. It does not simply
64 summarize the presentations and discussions at the Town Meeting, but tries to provide a broader context
65 and to present, in the words of the authors listed on the cover, a coherent picture of the status and future
66 of the field. [In formulating this text, the authors made extensive use not only of the presentations at the
67 Town Meeting, but also of additional material collected for the community white papers by the “Hot
68 QCD” and “Electron Ion Collider” communities [?, 1] whose scope is significantly more comprehensive
69 and to which the interested reader is directed for further details and additional projects.] Section 2 offers
70 an overview of the status, recent achievements, major open questions and future goals of research on the
71 “Phases of QCD Matter”, and describes how the above recommendations arise from such an overarching
72 view. Section 3 discusses in greater depth the science behind these future goals and what is needed to
73 successfully address the open questions listed in Section 2. Section 4 provides brief descriptions of the
74 science at and the design options for an Electron Ion Collider. Like our Recommendation #2 above,
75 the material provided in that section, although slightly rearranged, is identical in physical content with
76 a corresponding section in the “cold QCD” summary of the joint QCD Town Meeting, to reflect the
77 unanimous and strong support for the EIC project by the entire U.S. QCD Community. References and
78 an Appendix with the Town Meeting schedule are found at the end of this document.

2 Overview and Recommendations

2.1 Where we stand: recent insights and open questions

The bulk of the mass of the visible matter in the universe comes from energy stored in the strong interaction between its fundamental constituents. At a basic level, the strong interaction is well understood and described by Quantum Chromodynamics (QCD). Strongly interacting multi-particle systems feature numerous emergent phenomena that are difficult to predict from the underlying QCD theory, just like in condensed matter and atomic systems where the interactions are controlled by QED theory.

We now know that, as the universe evolved to its present state, strongly interacting matter existed in at least two distinct forms, a quark-gluon plasma (QGP) phase containing deconfined color charges that filled the universe homogeneously during its first few microseconds, and a clustered phase in which colored degrees of freedom are permanently confined into color-neutral objects called hadrons which make up the nuclei of today's atoms. Additional forms of strongly interacting matter that include a color superconducting phase may still exist in the cores of some compact stars or may have briefly existed in others before they collapsed into black holes. QCD matter is expected to have a complex phase diagram, possibly including one or more critical points.

The Relativistic Heavy Ion Collider (RHIC) at Brookhaven National Laboratory and the Large Hadron Collider (LHC) at CERN enable us to study strongly interacting matter at extreme temperatures in the laboratory. Conjectured over 35 years ago, the existence of the QGP phase was established unambiguously by experiments at RHIC which also made the surprising discovery that the QGP is strongly coupled and behaves like an almost perfect liquid. The successful implementation of luminosity and detector upgrades at the RHIC facility, recommended in the last Long Range Plan, and the beginning of the higher-energy heavy-ion program at the LHC in 2010 made additional studies possible that have begun to yield precise estimates for some of its key properties. Decisive theoretical progress at several fronts has been instrumental for these achievements. In response to a recommendation in the last Nuclear Physics Long Range Plan, the DOE made a dedicated investment into three Topical Collaborations in Nuclear Theory, among them the highly successful JET Collaboration. Both DOE and NSF have provided strong support for high performance computing. Facilitated by these initiatives, a standard framework has been developed and implemented that describes, with quantitative predictive power, the complete dynamical evolution of and the interaction of penetrating diagnostic probes with the expanding QCD matter created in heavy-ion collisions.

The unparalleled flexibility of the RHIC facility to collide atomic nuclei of different sizes over a wide range of energies, complemented by p+p, p+Pb and Pb+Pb collisions at the LHC with about 15 times the top RHIC energy, provides the experimental leverage necessary to clarify the nature of QCD matter. New discoveries made over the past decade have sharpened some questions and posed several new ones that address the core of our understanding of the nature, structure and origin of the QGP liquid. These questions frame our research program for the coming decade. To address them requires, in the short term, a suite of facility and detector upgrades at RHIC and the LHC and a series of new experiments that exploit these upgrades. In the long term they necessitate the construction of an Electron Ion Collider (EIC). The questions, in part motivated by recent discoveries summarized in the following subsection, are listed here and expanded upon in the science sections of this document:

- **What are the transport properties of the QGP? How do they change when the plasma is heated or doped with excess quarks?**
- **How do the collective properties of the QGP liquid, one of the most strongly coupled forms of matter now known, emerge from the interactions among the individual quarks**

123 and gluons that we know must be visible if the liquid is probed with sufficiently high
124 resolution?

- 125 • What is the precise nature of the initial state from which this liquid forms, and how does
126 it reach approximate local thermal equilibrium in the short time and rapidly expanding
127 environment provided by heavy-ion collisions?
- 128 • Can dense systems of quarks and gluons act like strongly coupled liquids without ther-
129 malizing? Does the Color Glass Condensate state that manifests itself when fast-moving
130 atomic nuclei are probed at very small longitudinal momentum fraction exhibit collective
131 behavior?
- 132 • What is the structure of the QCD phase diagram? Does it, like that of water, feature a
133 critical end point separating a line of first-order phase transitions at large baryon density
134 from the rapid but continuous crossover found by lattice QCD at low baryon density?
- 135 • How does the observed structure of the QGP change when it is probed at different length
136 scales, with photons, jets, and heavy quark flavors? What is the shortest length scale on
137 which the plasma liquid looks liquid-like?
- 138 • What is the smallest size and density of a droplet of QCD matter that behaves like a
139 liquid?

140 2.2 Accomplishments and future goals

141 We briefly summarize some recent achievements that play decisive roles in defining the research priorities
142 for the coming decade. Additional accomplishments and related future developments are described in the
143 science sections of this document.

144 Flow fluctuations and correlations

145 One of the most important recent breakthroughs has been the realization that each collision event (“Little
146 Bang”) exhibits its own unique flow pattern, with measurable strength up to the 7th or 8th multipole.
147 It was recently discovered that these ripples in the near-perfect QGP liquid bring information about
148 initial-state nucleonic and, likely, sub-nucleonic gluon fluctuations into the final state. This has opened
149 new possibilities to study the dense gluon fields and their quantum fluctuations in the colliding nuclei via
150 correlations between final state particles. Precise measurements of the complete set of measurable flow
151 coefficients, and their event-by-event fluctuations and correlations in both magnitude and flow angle, for
152 a number of identified hadron species will make it possible (in conjunction with the following item) to
153 map the transverse and longitudinal spatial dependence of the initial gluon fluctuation spectrum. This
154 will provide a test for QCD calculations in a high gluon density regime.

155 Quantifying the fluidity of quark-gluon plasma

156 Precise measurements of the flow coefficients up to the 5th and 6th multipole for charged hadrons, and
157 of elliptic and triangular flow for several identified hadron species, have made it possible to determine the
158 shear viscosity to entropy density ratio, η/s , of the QGP to within less than a factor of 2. This was only
159 possible with recently converged results from lattice QCD for the QCD equation of state and due to the
160 development of a comprehensive and sophisticated theoretical model for the dynamical evolution of the
161 collision, with relativistic viscous fluid dynamics to describe the QGP liquid at its core. A simultaneous
162 analysis of RHIC and LHC data has provided first evidence for an increase of $(\eta/s)_{\text{QGP}}$ with rising
163 temperature. The present uncertainty on $(\eta/s)_{\text{QGP}}$ (conservatively estimated as $\pm 50\%$) is not so much
164 limited by the quality of the available experimental data (which would be sufficient to determine the

165 viscosity with relative precision of 5-10%) as by the incompleteness of the presently available set of
166 measurements. It has recently been understood (see Sec. 3.1) that measurement of a complete set of
167 correlation functions between the momentum-dependent anisotropic flow coefficients and their associated
168 flow angles, for several particle species covering a wide range of masses, can not only tightly constrain the
169 spatial dependence of the initial gluon fluctuation spectrum but will also result in a large improvement in
170 our knowledge of the QGP transport coefficients.

171 The recent unexpected discovery of collective, anisotropic-flow signatures in p+Pb collisions at the
172 LHC and in a recent re-analysis of d+Au collisions at RHIC suggests that similar signatures seen in
173 very-high-multiplicity p+p collisions might also be of collective origin. How collectivity develops in such
174 small systems cries out for explanation. The inescapable last question on the list above can only be
175 answered systematically by exploiting RHIC's flexibility to collide atomic nuclei of any size over a wide
176 range of energies.

177 **Color opacity and temperature evolution of QCD matter from hard and penetrating probes**

178 **Parton energy loss and jet quenching:** Hard probes yield information about how energetic partons
179 diffuse in transverse momentum space and lose energy as they slice through strongly coupled QGP.
180 State-of-the-art analysis of the energy loss of leading hadrons in jets, together with significant recent
181 advances in theoretical modeling, both within perturbative QCD and by introducing insights from strong
182 coupling calculations, have increased the precision of our knowledge of the transverse momentum diffusion
183 parameter, \hat{q}/T^3 , by about an order of magnitude, to within a factor 2-3. The parton mass dependence
184 of jet modification and energy loss in heavy flavor jets will make it possible to separately quantify the
185 contributions from different energy-loss mechanisms. More generally, detailed studies of jet modification
186 by strongly coupled plasma over a wide range of angular and energy scales will connect its macroscopic
187 hydrodynamic description to a microscopic description in terms of quarks and gluons. As such, these
188 jet measurements will provide unique microscopic tools to move closer to a fundamental understanding
189 of how a strongly coupled liquid can arise in an asymptotically free gauge theory. Such measurements
190 require high luminosity operation and new instrumentation at RHIC and the LHC, and their quantitative
191 interpretation rests on further development of theoretical tools for a direct comparison of calculations to
192 the data.

193 **Quarkonium thermometry:** Precise and systematic measurements of quarkonium production can
194 determine the screening length of the static QCD force in a QGP. Screening effects are expected to be
195 easier to discern in bottomonium production, due to the absence of diluting effects from bottom quark
196 recombination. An initial observation of a significant suppression of the three Upsilon states in Pb+Pb
197 collisions at the LHC, indicating a sequential suppression pattern, was recently made by CMS; a precise
198 measurement will be available from the LHC by 2023. Low resolution and low statistics measurements have
199 been made by PHENIX and STAR and are consistent with the suppression of higher Upsilon states but the
200 different states could not be individually resolved. The statistical significance of STAR's measurements
201 will be improved over the next several runs and by 2021, the sPHENIX experiment will be making Upsilon
202 measurements at RHIC with both excellent mass resolution and much better statistical precision. The
203 combination of these data sets at quite different initial temperatures, together with the different sizes of
204 the three Upsilon states which provide measurements at three different length scales, will provide strong
205 constraints on the screening length in hot QCD matter.

206 **Electromagnetic probes:** Electromagnetic radiation from the Little Bangs integrates over the electro-
207 magnetic spectral function of hot QCD matter as it changes with position and time. This provides
208 information on the temperature evolution of the expanding fireball and opens a direct window on how
209 the degrees of freedom in the vector channel change with temperature. Pioneering measurements by

PHENIX have recently been augmented by first results from Pb+Pb collisions at the LHC and dilepton measurements at several collision energies by the STAR collaboration. These measurements were central in proving that the temperature achieved in heavy-ion collisions is the hottest ever man-made temperature. More precise future determinations of the low-mass dilepton spectrum are expected to lead to an improved understanding of chiral symmetry restoration at high temperature. Total yield and spectral slope measurements in the RHIC Beam Energy Scan (BES) program will help to quantitatively determine the changing fireball lifetime and temperature history at decreasing collision energy. Recently, unexpectedly large elliptic flows of direct photons measured by PHENIX and ALICE have presented the theory community with a puzzle. Its resolution requires more precise future measurements of the yields, slopes and anisotropic flow coefficients of direct photons at RHIC and LHC collisions.

Mapping the QCD phase diagram

Theoretical models suggest a phase diagram for QCD matter that rivals that of water in complexity. It is the only experimentally accessible phase diagram of matter that is controlled directly by the non-Abelian gauge field interactions in the fundamental forces of nature. Heavy-ion collisions at top RHIC and LHC energies produce strongly coupled plasma with a low value of μ_B where lattice QCD predicts a smooth crossover between the QGP liquid and a hadron resonance gas. Experimentally mapping the QCD phase diagram is one of the big unsolved challenges in the field. A first Beam Energy Scan (BES-I), with Au+Au collisions at center-of-mass energies between 39 and 7.7 GeV to explore QCD matter at baryon chemical potentials $110 \text{ MeV} \leq \mu_B \leq 420 \text{ MeV}$, was completed in 2014. BES-I led to a number of intriguing observations of non-monotonic beam energy dependences of several flow and fluctuation observables which might be connected with the appearance of a first-order phase transition at large μ_B . State-of-the-art lattice QCD calculations combined with dynamical modeling, using a hybrid approach that couples viscous fluid dynamics for the QGP liquid with a microscopic approach to the critical phase transition dynamics and the subsequent evolution of the hadronic phase, will be required to test these interpretations. A second Beam Energy Scan (BES-II) planned for 2018-2019, with significantly improved beam luminosity and upgraded detector capabilities, and concurrent improvements of the theoretical modeling at lower beam energies are needed to solidify the suggestive results from BES-I with precision measurements in the targeted energy region identified in BES-I. Unambiguous discovery of a critical point in BES-II would warrant additional measurements at a later time to further quantify its properties.

Forward rapidity studies at high energy and the Color Glass Condensate

Both RHIC and the LHC are capable of probing new, unmeasured physics phenomena at low longitudinal momentum fraction x . Data from the 2013 p+Pb run at the LHC will make it possible to study previously unreachable phase-space in the search for parton saturation effects (the Color Glass Condensate). Forward-rapidity detector upgrades in STAR and PHENIX will open the door to studies of saturation physics at RHIC. However, a complete exploration of parton dynamics at low x will require an Electron Ion Collider (EIC). While a future EIC will deliver crucially missing precise information on the nuclear parton distribution functions in a kinematic regime where in heavy-ion collisions saturation effects are difficult to separate from QGP physics, forward rapidity studies in p+A and A+A collisions at RHIC and LHC provide access to low- x physics in a complementary kinematic range.

2.3 Recommendations

2.3.1 New questions and opportunities in relativistic heavy-ion collisions

Over the past decade, through a panoply of measurements made in heavy-ion collisions at the Relativistic Heavy Ion Collider (RHIC) and the Large Hadron Collider (LHC), in concert with theoretical advances

253 coming from calculations done using many different frameworks, we have obtained a broad and deep
254 knowledge of what hot QCD matter does, but we still know little about how it works. These collisions
255 create exploding little droplets of the hottest matter seen anywhere in the universe since it was a few
256 microseconds old. We have increasingly quantitative empirical descriptions of the phenomena manifest in
257 these explosions, and of some key material properties of the matter created in these “Little Bangs” which
258 turns out to be a strongly coupled liquid. However, we still do not know the precise nature of the initial
259 state from which this liquid forms, and know very little about how the properties of this liquid vary across
260 its phase diagram or how, at a microscopic level, the collective properties of this liquid emerge from the
261 interactions among the individual quarks and gluons that we know must be visible if the liquid is probed
262 with sufficiently high resolution.

263 Answering these and other questions requires an intensive modeling and computational effort to simulta-
264 neously determine the set of key parameters needed for a multi-scale characterization of the QGP medium
265 and the initial state from which it emerges. This phenomenological effort requires broad experimental
266 input from a diverse set of measurements, including 1) the completion of the heavy quark program to
267 measure the diffusion coefficient of heavy quarks, 2) energy scans to map the phase diagram of QCD and
268 the dependence of transport coefficients on the temperature and baryon number chemical potential, 3)
269 collisions of nuclei with varied sizes, including p+A and very high multiplicity p+p collisions, to study the
270 emergence of collective phenomena, 4) the quantitative characterization of the electromagnetic radiation
271 emitted by the Little Bangs and its spectral anisotropies, and 5) a detailed investigation at RHIC and
272 LHC of medium effects on the production rates and internal structure of jets of hadrons, for multi-scale
273 tomographic studies of the medium. These considerations lead us to our

Recommendation #1:

274 **The discoveries of the past decade have posed or sharpened questions that are central to understanding the nature, structure, and origin of the hottest liquid form of matter that the universe has ever seen. As our highest priority we recommend a program to complete the search for the critical point in the QCD phase diagram and to exploit the newly realized potential of exploring the QGP’s structure at multiple length scales with jets at RHIC and LHC energies. This requires**

- **implementation of new capabilities of the RHIC facility (a state-of-the-art jet detector such as sPHENIX and luminosity upgrades for running at low energies) needed to complete its scientific mission,**
- **continued strong U.S. participation in the LHC heavy-ion program, and**
- **strong investment in a broad range of theoretical efforts employing various analytical and computational methods.**

275 RHIC and the LHC, together, provide an unprecedented opportunity to study the properties of QCD
276 matter. While collisions at the LHC create temperatures well above those needed for the creation of
277 QGP and may thus be able to explore the expected transition from a strongly coupled liquid to a weakly
278 coupled gaseous phase at higher temperatures, the RHIC program enables unique research at temperatures
279 close to the phase transition. Moreover, the unparalleled flexibility of RHIC makes possible collisions
280 between a variety of different ion species over a broad range in energy. The combined programs permit
281 a comprehensive exploration of the QCD phase diagram, together with precise studies of how initial
282 conditions affect the creation and dynamical expansion of hot QCD matter and of the microscopic
283 structure of the strongly coupled QGP liquid.

2.3.2 A precision femtoscope to study the glue that binds us all

It is generally believed that, at high energies, interacting gluon fields from the colliding hadrons dominate the energy deposition in the collision zone and the subsequent thermalization processes that eventually lead to the creation of a quark-gluon plasma. The possibility to precisely measure the gluon wave functions of the incoming nuclei, in order to complement the empirical determination of the gluonic initial state from flow fluctuations and correlations in heavy-ion collisions, is expected to further solidify the determination of the key parameters characterizing the thermodynamic and transport properties of the QGP. The construction of an Electron Ion Collider (EIC) will address this need.

The EIC will image the gluons and sea quarks in the proton and nuclei with unprecedented precision and probe their many-body correlations in detail, providing access to novel emergent phenomena in QCD. It will definitively resolve the proton's internal structure, including its spin, and explore a new QCD frontier of ultra-dense gluon fields in nuclei at high energy. These advances are made possible by the EIC's unique capability to collide polarized electrons with polarized protons and light ions at unprecedented luminosity and electrons with heavy nuclei at high energy. An EIC will be absolutely essential to maintain U.S. leadership in fundamental nuclear physics research in the coming decades:

Recommendation #2:

A high luminosity, high-energy polarized Electron Ion Collider (EIC) is the U.S. QCD community's highest priority for future construction.

2.3.3 New initiatives to further strengthen nuclear theory

Due to the complexity of heavy-ion collision dynamics, the success of the research program outlined in this document hinges on continued strong support of a broad range of theoretical activities. In addition to a healthy base program, the field requires specific support in high-performance computing and of collaborative efforts focused on addressing complex issues that need contributions from several scientists or groups of scientists with complementary expertise. Examples for the first need are the determination of thermal equilibrium properties and response functions of the QGP from lattice QCD, the dynamical simulation of the thermalization processes in the initial stage of heavy-ion collisions, and comprehensive model/data comparisons involving large data sets and complex dynamical models that aim at extracting key model parameters with quantified uncertainties. An example for the latter is the DOE-funded JET Topical Collaboration that addresses the problem of turning measurements of the medium modification of jets and electromagnetic probes into precise tomographic tools that yield quantitative information about the properties and dynamical evolution of the dense QCD matter created in heavy-ion collisions.

The high-performance computing needs of the nuclear theory community were addressed at a Town Meeting in Washington, D.C., on July 14-15, 2014, which passed the following recommendation and request:

Recommendation: Realizing the scientific potential of current and future experiments demands large-scale computations in nuclear theory that exploit the US leadership in high-performance computing. Capitalizing on the pre-exascale systems of 2017 and beyond requires significant new investments in people, advanced software, and complementary capacity computing directed toward nuclear theory.

Request: To this end, we ask the Long-Range Plan to endorse the creation of an NSAC subcommittee to develop a strategic plan for a diverse program of new investments in computational nuclear theory. We expect this program to include:

- new investments in SciDAC and complementary efforts needed to maximize the impact of the

- 324 experimental program;
- 325 • development of a multi-disciplinary workforce in computational nuclear theory;
 - 326 • deployment of the necessary capacity computing to fully exploit the nations leadership-class
 - 327 computers.

328 At the QCD Town Meeting at Temple University, the “Phases of QCD Matter” subcommunity endorsed
329 this resolution and amended it as follows:

330

Recommendation #3:

331

We endorse the new initiatives and investments proposed in the Recommendation and Request received from the Computational Nuclear Physics Town Meeting, at a level to be determined by the requested NSAC subcommittee. In addition, we recommend new funding to expand the successful “Topical Collaborations in Nuclear Theory” program initiated in the last Long Range Plan of 2007, to a level of at least one new Topical Collaboration per year.

332 **2.3.4 Educating and mentoring the next generation of scientists**

333 A continuous pipeline of highly and broadly educated young scientists is not only the lifeblood of the
334 U.S. Nuclear Science program, but also a guarantor of our nation’s continued technological and economic
335 strength and its ability to innovate. At a separate Town Meeting dedicated to Education and Innovation
336 (Michigan State University, August 6-8, 2014) the following resolutions were passed:

- 337 1. Education and mentoring of the next generation nuclear scientists as well as dissemination of
338 research results to a broad audience should be recognized by all researchers as an integral part of
339 the scientific enterprise.
- 340 2. Nuclear science is an active and vibrant field with wide applicability to many societal issues. It is
341 critical for the future of the field that the whole community embraces and increases its promotion
342 of nuclear science to students at all stages in their career as well as to the general public.
- 343 3. Researchers in nuclear physics and nuclear chemistry have been innovative leaders in the full
344 spectrum of activities that serve to educate nuclear scientists as well as other scientists and the
345 general public in becoming informed of the importance of nuclear science. The researchers are
346 encouraged to build on these strengths to address some of the challenges in educating an inclusive
347 community of scientists as well as those on the path to future leadership in nuclear science.
- 348 4. The interface between basic research in nuclear physics and exciting innovations in applied nuclear
349 science is a particularly vital component that has driven economic development, increased national
350 competitiveness, and attracts students into the field. It is critical that federal funding agencies
351 provide and coordinate funding opportunities for innovative ideas for potential future applications.

352 In separate sessions at the QCD Town Meeting at Temple University, the “Phases of QCD Matter” and
353 “QCD and Hadron Structure” subcommunities voted unanimously for the following

Recommendation #4:

354

The QCD community endorses and supports the conclusions from the Education and Innovation Town Meeting.

3 Quantifying the Properties of QCD Matter – Present Status and Future Opportunities

3.1 Completing the Little Bang Standard Model

One of the most important recent discoveries in heavy-ion collisions is that density fluctuations from the initial state of heavy-ion collisions survive through the expansion of the fireball showing up as correlations between produced particles [2–10]. Prior work had mostly approximated the incoming nuclei as smooth spheres and the initial overlap region as an ellipse. The survival of density and geometry fluctuations was first hinted at in measurements of cumulants related to shape of the v_2 distribution [11, 12]. The picture started to become more clear after measurements were made in Cu+Cu collisions where the fluctuations were more prominent in the smaller system [13]. Ultimately, a new paradigm emerged as the structure of the initial state was found to play a central role in two-particle correlation functions and the previous measurements of v_2 were generalized to v_n , a spectrum carrying information about both the initial densities in the collision as well as the dissipative properties of the subsequent plasma phase [14]. The survival of the initial state fluctuations is intimately related to the earlier finding that the QGP discovered at RHIC is the most perfect fluid known [15–17], with a viscosity to entropy density ratio η/s near the string theory bound [18]. The low viscosity plasma phase acts as a lens (albeit of strongly non-linear character), faithfully transferring the geometric structure of the initial density distributions, with its associated distribution of pressure gradients which act as a hydrodynamic force, into the final state. There it shows up most prominently as correlations between produced particles. Quantum fluctuations in the initial state cause these correlations to fluctuate from event to event.

Descriptions of these new phenomena have required the development of a new dynamical framework for heavy-ion collisions. It includes i) modeling of initial-state quantum fluctuations of nucleon positions and sub-nucleonic color charges and the color fields generated by them, ii) a description of the pre-equilibrium dynamics that evolves the initial energy-momentum tensor by solving either the (2+1)-dimensional Yang-Mills equations for the gluon fields (weakly-coupled approach) or Einstein’s equations of motion in five-dimensional anti-deSitter space (strongly-coupled approach), followed by iii) the rapid transition, event-by-event, to second-order viscous relativistic fluid dynamics, and iv) a late-stage hadron phase described by microscopic transport calculations. While there is widespread agreement on the general structure of such a standardized dynamical approach, it has not yet reached the level of uniqueness that would justify calling it the “Little Bang Standard Model” [19]. Model comparisons with experimental data that illustrate the state of the art in dynamical modeling can be found in [17, 20–28]. With the existence of a reliable equation of state from lattice QCD calculations [29–32] a crucial degree of uncertainty in hydrodynamic modeling could be eliminated, enabling the development of a complete hydrodynamic space-time model. With this full space-time picture in hand, the comparisons of model calculations to harmonic decompositions of correlation functions ($\sqrt{v_n^2}$) at RHIC and the LHC (shown in Fig. 1) have reduced the uncertainty on η/s by a factor of 10 [33]. With this newfound precision, studies suggest that η/s is smaller for RHIC collisions (right panel of Fig. 1) than it is at the LHC (left panel), consistent with a temperature dependent η/s with a minimum near the critical temperature. In the next phase of study we seek to 1) accurately determine the temperature dependence of η/s (aided by the Beam Energy Scan Program at RHIC) and 2) develop a clearer picture of the high density gluon fields that form the precursor of the plasma phase (aided by the p+A program and ultimately by an Electron Ion Collider).

So what is needed to turn this standard dynamical framework into the “Little Bang Standard Model”? One fundamental challenge along the way is the need to determine *simultaneously* the space-time picture of the collective expansion and the medium properties that drive this expansion [19]. A unique and reliable

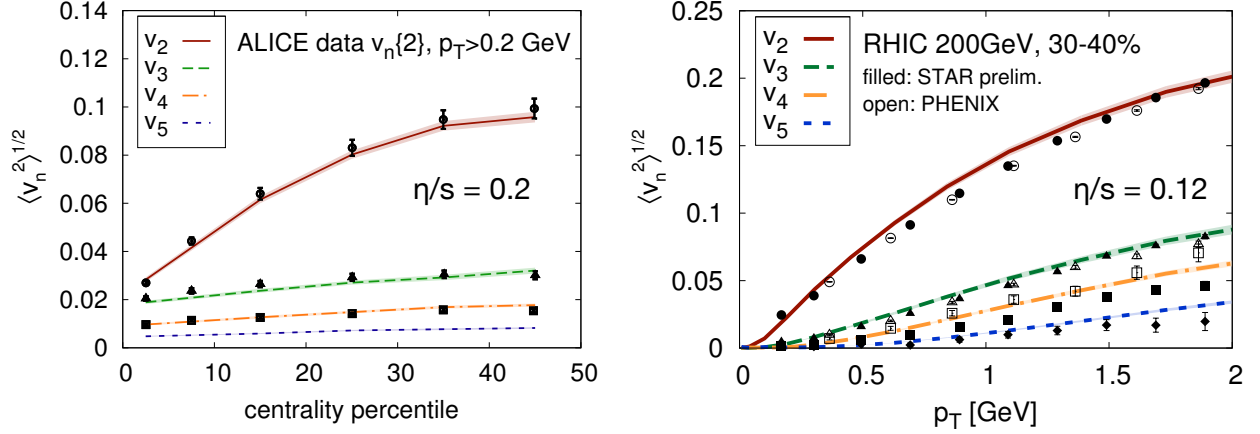


Figure 1: Model calculations compared to measurements of the harmonic decomposition of azimuthal correlations produced in heavy-ion collisions. The left panel shows model calculations and data for v_n vs. collision centrality in Pb+Pb collisions at $\sqrt{s_{\text{NN}}} = 2.76$ TeV. The right panel shows similar studies for the p_T dependence of v_n in 200 GeV Au+Au collisions. The comparison of the two energies provides insight on the temperature dependence of η/s .

399 determination of these two unknowns is aided by measurements of multiple flow observables sensitive
 400 to medium properties in different stages of the evolution [14, 34, 35]. Due to the large event-by-event
 401 fluctuations in the initial state collision geometry, in each collision the created matter follows a different
 402 collective expansion with its own set of flow harmonics (magnitude v_n and phases Φ_n). Experimental
 403 observables describing harmonic flow can be generally given by the joint probability distribution of the
 404 magnitudes v_n and phases Φ_n of flow harmonics:

$$p(v_n, v_m, \dots, \Phi_n, \Phi_m, \dots) = \frac{1}{N_{\text{evts}}} \frac{dN_{\text{evts}}}{dv_n dv_m \dots d\Phi_n d\Phi_m}. \quad (1)$$

405 Specific examples include the probability distribution of individual harmonics $p(v_n)$, flow de-correlation
 406 in transverse and longitudinal directions, and correlations of amplitudes or phases between different
 407 harmonics ($p(v_n, v_m)$ or $p(\Phi_n, \Phi_m)$). The latter are best accessed through measurements of correlations
 408 with three or more particles. The joint probability distribution (1) can be fully characterized experimentally
 409 by measuring the complete set of moments recently identified in Ref. [36]. With the added detail provided
 410 by these measurements, hydrodynamic models can be fine-tuned and over-constrained, thus refining
 411 our understanding of the space-time picture and medium properties of the heavy-ion collisions. Initial
 412 measurements of some of these observables [37–39] and comparison to hydrodynamic models [24, 40–42]
 413 already provided unprecedented insights on the nature of the initial density fluctuations and dynamics of
 414 the collective evolution.

415 The agreement between the model and the data shown in Figure 1 suggests that the essential features
 416 of the dynamic evolution of heavy-ion collisions are well described by current models. These model
 417 calculations depend on a significant number of parameters that are presently poorly constrained by
 418 fundamental theory, and a reliable determination of the QGP properties requires a systematic exploration
 419 of the full parameter space. An example of such an exploration [43] is shown in Figure 2 where the
 420 shape of the QCD EOS is treated as a free parameter. The left panel shows a random η sample of the
 421 thousands of possible Equations of State, constrained only by results on the velocity of sound obtained by
 422 perturbative QCD at asymptotically high temperature and by lattice QCD at the crossover transition
 423 temperature. They are compared to the EOS determined from lattice QCD [32]. The right panel shows a

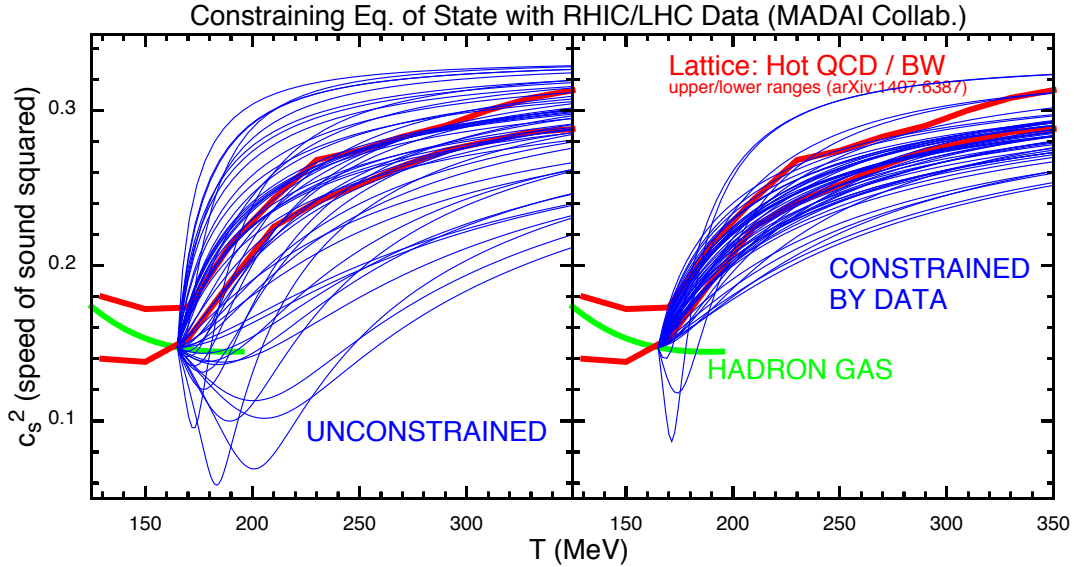


Figure 2: The QCD Equation of State (more precisely: the squared speed of sound, c_s^2 , as a function of temperature) from lattice QCD calculations and from models constrained by data from RHIC and the LHC. The red lines delimit the present uncertainty range of c_s^2 from lattice QCD. The blue lines show a number of parametrizations of $c_s^2(T)$; in the left panel, they are constrained only by their asymptotic values at $T = 165 \text{ MeV} \simeq T_c$ and $T = \infty$, in the right panel they are additionally required to provide an acceptable fit to experimental data as described in [43]. The right panel shows that experimental data give preference to an Equation of State consistent with lattice QCD. This demonstrates that our model of the collision dynamics is good enough to allow us to study emergent properties in QCD matter.

424 sample of the Equations of State allowed by experimental data. The results of this study suggest that
 425 data at RHIC and the LHC require an EOS consistent with that expected from QCD. This demonstrates
 426 that our model of heavy-ion collisions describes the dynamics of the collisions well enough that we can
 427 extract information on the emergent properties of finite temperature QCD from the experimental traces
 428 left by the tiny droplet of QGP created in the collisions. These state-of-the-art models can therefore be
 429 used to both determine properties of finite temperature QCD currently inaccessible to lattice calculations
 430 and to provide an accurate space-time profile needed for modeling other processes like jet quenching.
 431 Figure 3 shows a schematic representation of our current uncertainty on the temperature dependence of
 432 η/s in QCD matter. While many of the existing measurements are accurate enough, as seen in Fig. 1,
 433 to determine η/s with much greater precision *if all other model parameters were already known*, the
 434 non-linear simultaneous dependence of the observables on multiple parameters does not yet allow one to
 435 translate the high quality of these experimental data into a more precise estimate of η/s . The studies
 436 shown in Figures 2 and 1 suggest, however, that a more complete set of measurements of the moments
 437 of the joint probability distribution (1) at the LHC and RHIC (particularly in the Beam Energy Scan),
 438 coupled with extensive quantitative modeling, will provide the desired access to $(\eta/s)(T)$ in and around
 439 the transition temperature where hadrons melt into a Quark Gluon Plasma, and strongly reduce the width
 440 of the blue uncertainty band in Fig. 3.

441 The temperature dependence of η/s can be further constrained by measuring directly emitted photons
 442 and dileptons. Their lack of strong interactions makes them penetrating probes that reflect the medium
 443 properties at the time of their emission which, on average, precedes that of the much more abundant
 444 strongly interacting hadrons. The slopes of their transverse momentum spectra and their anisotropic flow

445 coefficients therefore show sensitivity to the hydrodynamic flow and dissipative medium properties at
 446 higher average temperature than the corresponding hadronic observables [44, 45]. Recent elliptic and
 447 triangular flow measurements of direct photons in Au+Au collisions at RHIC [46] and Pb+Pb collisions
 448 at the LHC [47] have presented a puzzle to theorists because the measured flow anisotropies are much
 449 larger than theoretically predicted [44, 45]. This may point to stronger electromagnetic radiation from
 450 the critical crossover region between the QGP and hadronic phases [48] than presently thought. Future
 451 higher-luminosity runs and improved detector capabilities will provide much more precise data for these
 452 very difficult measurements. In concert with state-of-the-art dynamical modeling, this is expected to not
 453 only yield a resolution of this “direct photon flow puzzle” but also lead to tighter constraints on the
 454 transport properties of QCD matter at higher temperatures.

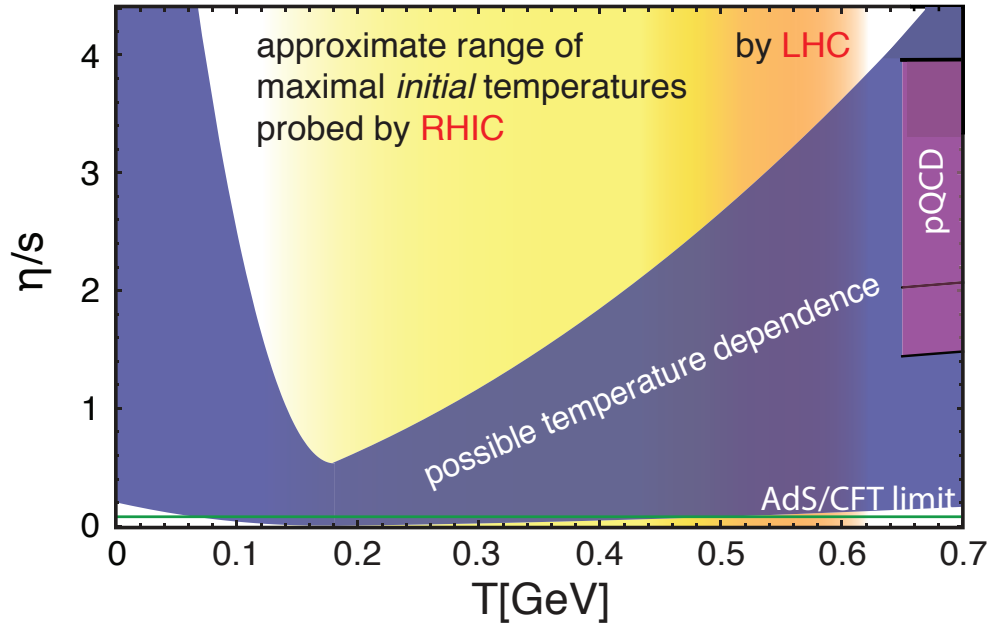


Figure 3: The temperature dependence of the specific viscosity η/s . The blue band represents the range allowed by our current understanding based on comparing experimental data to models with a minimum at the transition temperature. pQCD calculations and the string theory lower bound are also shown. The shaded vertical regions represent the ranges of initial temperatures probed by RHIC and the LHC.

455 Completion of the Little Bang Standard Model will also require a better understanding of the gluon
 456 densities in the initial overlap regions. As discussed in sections 3.4 and 4, this topic can be studied in p+A
 457 collisions and ultimately at an electron ion collider (EIC). The physics of p+A collisions has proven to be
 458 richer than originally anticipated. While collective flow phenomena are firmly established in sufficiently
 459 central collisions of heavy nuclei, these effects were not expected in p+p and p+A collisions. It was
 460 widely assumed that, as the mean-free-path of the matter approaches the characteristic size of the system,
 461 the effects of viscous damping would become too strong and invalidate a hydrodynamic description.
 462 Surprisingly, correlations that are long-range in rapidity and similar to those measured in A+A collisions
 463 have now also been observed at the LHC in rare high-multiplicity p+p collisions [49] (corresponding to
 464 high gluon-density initial states). Subsequent measurements revealed similar phenomena at both the LHC
 465 and RHIC in high multiplicity p+Pb [50–52] and d+Au [53] collisions. In particular, the observed mass
 466 ordering of the spectral slopes [54–57] and of $v_n(p_T)$ [58, 59] is reminiscent of the effects arising from a
 467 common radial flow boost in A+A collisions. Multi-particle measurements [60] show unambiguously that
 468 the correlations in high-multiplicity p+Pb collisions are collective.

469 Understanding the relationship between initial and final-state effects in these systems appears to be
470 non-trivial and has now developed into a very active research area. While hydrodynamic models with
471 strong final-state interactions may provide a natural interpretation for many of the observed features,
472 their applicability in such small systems, including the process of rapid thermalization, requires additional
473 scrutiny [61]. Meanwhile, other novel mechanisms, exploiting quark and gluon momentum correlations in
474 the initial state, have been proposed as alternative interpretations of the observed long-range correlations
475 and even predicted the correlation results in p+p collisions. Recently collected data from ${}^3\text{He}+\text{Au}$
476 collisions will shed additional light on this question, as will improved correlation measurements at forward
477 rapidity, enabled by current and future detector upgrades. These programs play an important role in
478 1) understanding the initial-state component of our Little Bang Standard Model and its subsequent
479 modification by final-state interactions, 2) testing how small a system can be and still exhibit fluid-like
480 phenomena, 3) providing new opportunities to probe the spectrum of fluctuations in high gluon density
481 matter, and 4) mapping the transition to a classical description of gluonic matter at high density.

482 It is suspected that the rapid formation of almost perfectly liquid hot QCD matter in heavy-ion collisions
483 may be related to the emergence of universal characteristics in high-density gluon matter at zero
484 temperature that is predicted to dominate the low- x component of the nuclear wave function when probed
485 at high energy. To explore this connection, precision measurements of the nuclear wave function at an
486 EIC will be required to complement nuclear collision experiments with small and large nuclei.

487 3.2 Mapping the QCD phase diagram

488 When the first protons and neutrons and pions formed in the microseconds-old universe, and when they
489 form in heavy-ion collisions at the highest RHIC energies and at the LHC, they condense out of liquid
490 quark-gluon plasma consisting of almost as much antimatter as matter. Lattice calculations [62–64] show
491 that QCD predicts that, in such an environment, this condensation occurs smoothly as a function of
492 decreasing temperature, with many thermodynamic properties changing dramatically but continuously
493 within a narrow temperature range around the transition temperature $T_c \in [145 \text{ MeV}, 163 \text{ MeV}]$ [32, 64],
494 referred to as the crossover region of the phase diagram of QCD, see Fig. 4. In contrast, quark-gluon
495 plasma doped with a sufficient excess of quarks over anti-quarks may instead experience a sharp first
496 order phase transition as it cools, with bubbles of quark-gluon plasma and bubbles of hadrons coexisting
497 at a well-defined critical temperature, much as bubbles of steam and liquid water coexist in a boiling
498 pot. The point where the doping of matter over antimatter (parametrized by the net baryon number
499 chemical potential μ_B) becomes large enough to instigate a first order phase transition is referred to
500 as the QCD critical point. It is not yet known whether QCD has a critical point [65–69], nor where
501 in its phase diagram it might lie. Lattice calculations become more difficult or more indirect or both
502 with increasing μ_B and, although new methods introduced within the past decade have provided some
503 hints [66, 68, 70], at present only experimental measurements can answer these questions definitively. The
504 theoretical calculations are advancing, however, with new methods and advances in computational power
505 both anticipated.

506 The phase diagram of QCD, with our current knowledge schematically shown in Fig. 4, is the only
507 phase diagram of any form of matter in Nature that we have a chance of both mapping experimentally
508 and relating directly and quantitatively to our fundamental description of Nature, the Standard Model.
509 With QCD the only strongly interacting theory in the Standard Model, mapping the transition region
510 of its phase diagram is a scientific goal of the highest order. In the long term, successfully connecting
511 a quantitative, empirical understanding of its phases and the transitions between phases to theoretical
512 predictions obtained from the QCD Lagrangian could have ramifications in how we understand phases of

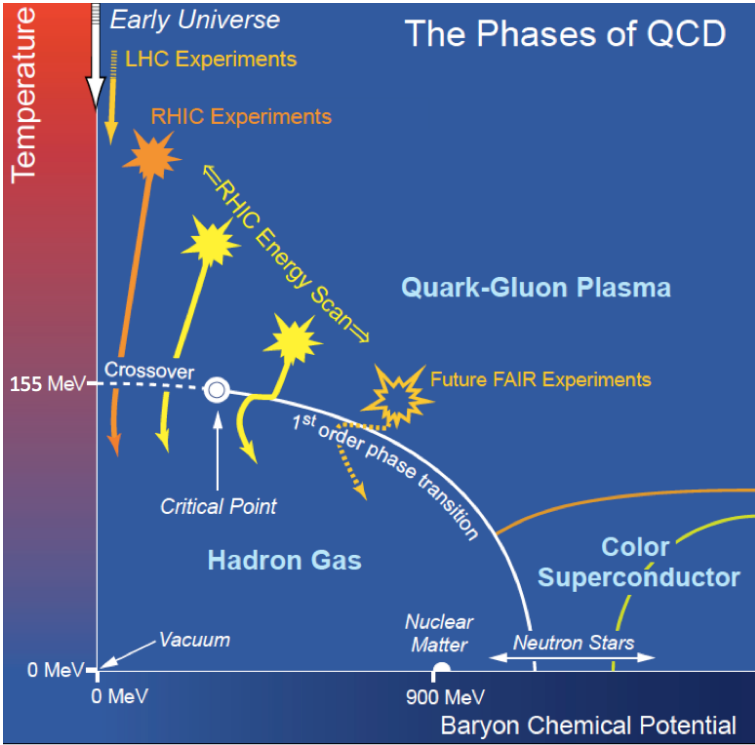


Figure 4: A sketch illustrating the experimental and theoretical exploration of the QCD phase diagram. Although experiments at highest energies and smallest baryon chemical potential are known to cross from a QGP phase to a hadron gas phase through a smooth crossover, lower energy collisions can access higher baryon chemical potentials where a first order phase transition line is thought to exist.

513 strongly coupled matter in many other contexts.

514 **RHIC’s unique capability to probe the QCD phase diagram**

515 A major effort to use heavy-ion collisions at RHIC to survey the phase diagram of QCD is now underway.
 516 The excess of matter over antimatter in the exploding droplet produced in a heavy-ion collision can be
 517 increased by decreasing the collision energy, which reduces the production of matter-antimatter symmetric
 518 quark-antiquark pairs and gluons relative to the quarks brought in by the colliding nuclei, thus increasing
 519 μ_B . Decreasing the collision energy also decreases the maximum, i.e. initial, temperature reached by
 520 the matter produced in the collision. A series of heavy-ion collision measurements scanning the collision
 521 energy [71] can therefore explore the properties of matter in the crossover region of the phase diagram,
 522 matter that is neither quark-gluon plasma nor hadronic or both at the same time, as a function of the
 523 doping μ_B . Such a program can scan the transition region of the QCD phase diagram out to μ_B values
 524 that correspond to collision energies below which the initial temperature no longer reaches the transition.
 525 If the crossover region narrows to a critical point within this experimentally accessible domain, an energy
 526 scan can find it. RHIC completed the first phase of such an energy scan in 2014, taking data at a series
 527 of energies ($\sqrt{s_{NN}} = 200, 62.4, 39, 27, 19.6, 14.5, 11.5$ and 7.7 GeV) corresponding to values of μ_B that
 528 range from 20 to 400 MeV. Data from these experiments at RHIC [71, 72] and from previous experiments
 529 confirm that lower-energy collisions produce QGP with higher μ_B , as anticipated. A selection of data
 530 from BES-I that exhibit interesting non-monotonic behavior as a function of collision energy is shown in
 531 Fig. 5.

532 RHIC is, and will remain, the optimal facility in the world for studying matter in the crossover region
 533 and searching for a possible critical point in the so far less well understood regions of the phase diagram
 534 with larger μ_B . What makes RHIC unique is both its wide reach in μ_B and that it is a collider, meaning
 535 that the acceptance of detectors, and hence the systematics of making measurements, change little as a
 536 function of collision energy. Accelerator and detector performance has been outstanding during the first

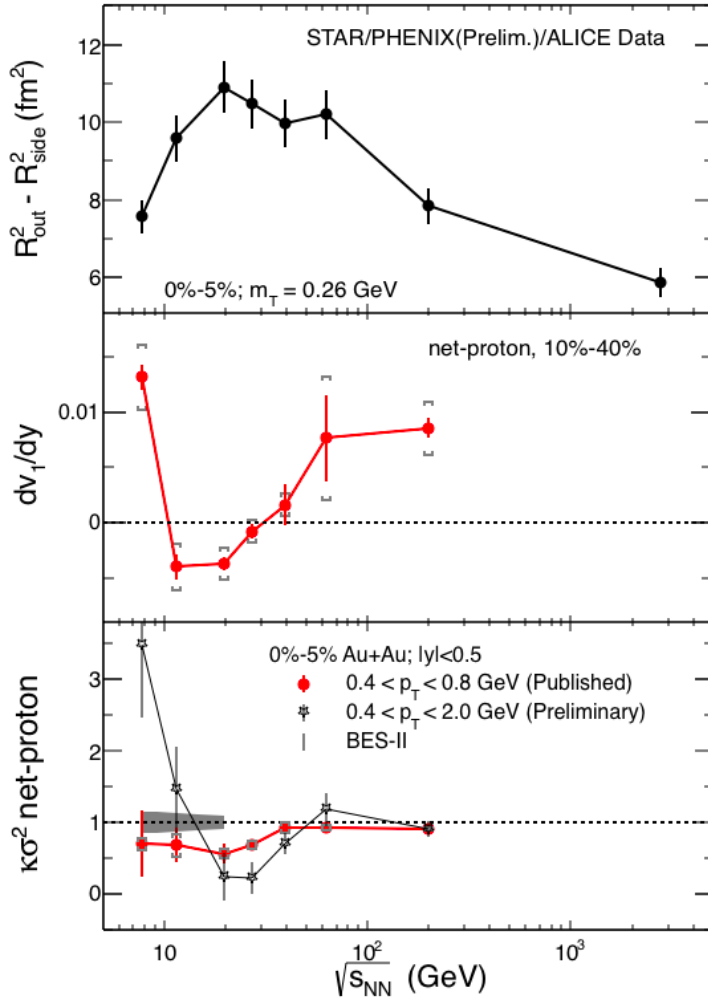


Figure 5: Three selected observables that all show interesting non-monotonic behavior as functions of collision energy around $\sqrt{s_{NN}} \sim 15\text{--}20$ GeV.

Top panel: $R_{out}^2 - R_{side}^2$, measured via two-pion interferometry by STAR [73], PHENIX [74], and ALICE [75], reflects the lifetime of the collision fireball. $R_{out}^2 - R_{side}^2$ was predicted [76] to reach a maximum for collisions in which the hydrodynamic fluid forms at temperatures where the equation of state is softest.

Middle panel: The rapidity-slope of the net proton directed flow v_1 , dv_1/dy . This quantity is sensitive to early pressure fields in the medium.

Bottom panel: The kurtosis of the event-by-event distribution of the net proton (i.e. proton minus antiproton) number per unit of rapidity, normalized such that Poisson fluctuations give a value of 1. In central collisions, published results in a limited kinematic range [77] show a drop below the Poisson baseline around $\sqrt{s_{NN}} = 27$ and 19.6 GeV. New preliminary data over a larger p_T range [78], although at present with substantial uncertainties, hint that the normalized kurtosis may, in fact, rise above 1 at lower $\sqrt{s_{NN}}$, as expected from critical fluctuations [79]. The grey band shows the much reduced uncertainties anticipated from BES-II in 2018-2019, for the 0-5% most central collisions.

537 phase of this program, referred to as Beam Energy Scan I or BES-I. Measurements of all the important
 538 observables targeted in the planning of this campaign have now been made in collisions with energies
 539 varying by a factor of 25, allowing for a first look at a large region of the phase diagram of QCD.

540 **The need for BES-II and accompanying advances in theory**

541 We still await with interest the results from the most recent run in this program at $\sqrt{s_{NN}} = 14.5$ GeV, where
 542 data were taken only a few months ago; and for a number of important observables the measurements
 543 made at and below $\sqrt{s_{NN}} = 19.6$ GeV have quite limited statistics. Nevertheless, it is already possible
 544 to see trends and features in the data that provide compelling motivation not only for a strong and
 545 concerted theoretical response aiming at quantitative precision, but also for much higher statistics data
 546 at the lower end of the energy range (i.e. at the largest achievable values of μ_B) that will be provided by
 547 the second phase of the Beam Energy Scan program (BES-II) in 2018 and 2019. The goals of BES-II, as
 548 described in more detail below, are to follow through and turn trends and features into definitive scientific
 549 conclusions. To this end, the accelerator physicists at RHIC are planning a machine upgrade to provide
 550 electron cooling to increase the beam luminosity at these energies by about a factor 10 [71]. Targeted
 551 new detector capabilities will also increase the sensitivity to the signals described below in the BES-II
 552 campaign [71].

553 Experimental discovery of a first order phase transition or a critical point on the QCD phase diagram
554 would be a landmark achievement. The first goals of the BES program, however, relate to obtaining a
555 quantitative understanding of the properties of matter in the crossover region of the phase diagram as it
556 changes with increasing μ_B . Available tools developed over the last few years now make a quantitative
557 comparison between theory and experiment tractable in the μ_B -range below any QCD critical point.
558 Success in this, in and of itself, would constitute a major and lasting impact of the RHIC program.
559 Questions that can be addressed in this regime include quantitative study of the onset of various signatures
560 associated with the presence of quark-gluon plasma and of the onset of chiral symmetry restoration as
561 one traverses the crossover region. Data now in hand from BES-I provide key inputs and impetus toward
562 this goal. Here we give four examples, intended to be illustrative, of areas where a coherent experimental
563 and theoretical effort is expected to have substantial impact on our understanding of QCD. In each case
564 we also note the substantial impact expected from the additional measurements anticipated during the
565 BES-II:

566 **1.** The directed flow observable dv_1/dy for net protons has been found to feature a dip as a function of
567 collision energy (see middle panel in Fig. 5), with a minimum at energies somewhere between $\sqrt{s_{NN}} = 11.5$
568 and 19.6 GeV [80]. This has long been predicted in qualitative terms as a consequence of the softening of
569 the equation of state in the transition region of the phase diagram [81, 82]. Several theoretical groups
570 around the world have now begun hydrodynamic calculations with nonzero baryon density, deploying all the
571 sophistication that has been developed very recently in the analysis of higher energy collisions, including
572 initial fluctuations and a hadronic afterburner, in applications to these lower energy collisions. These
573 hydrodynamic+hadronic cascade calculations will be used to compare the dv_1/dy data with equations of
574 state in the crossover region of the phase diagram obtained from lattice calculations via Taylor expansion
575 in μ_B/T [83]. This is a program where a quantitative comparison, successful or not, will be of great
576 interest, since failure to describe the data could signal the presence of a first order phase transition.
577 The precision of a comparison like this will be substantially improved in 2018-19 when BES-II data will
578 allow dv_1/dy to be measured for the first time with tightly specified centrality; the statistics available in
579 the BES-I data sets limit present measurements to averages over collisions with widely varying impact
580 parameters [80].

581 **2.** A second goal of the hydrodynamic calculations referred to above will be to use identified particle
582 BES-I v_2 data to map, in quantitative terms, where and how hydrodynamics starts to break down at
583 lower collision energies, and where, to an increasing extent, v_2 develops during the hadron gas phase
584 when viscosities are not small, i.e. where the contribution of the partonic phase to observed measures of
585 collectivity decreases in importance. A key future experimental input to this program is the measurement
586 of the elliptic flow v_2 of the ϕ -meson, which will be obtained with substantially greater precision in the
587 BES-II program. The first measurements of v_2 of Ω baryons at these collision energies, also anticipated
588 in BES-II, will represent a further, substantial advance. Seeing ϕ mesons flowing like lighter mesons and
589 Ω baryons flowing like lighter baryons in collisions at a given energy would indicate that the dominant
590 contribution to the collective flow in those collisions was generated during the partonic phase [84].

591 This component of the BES program, together with the following one, will yield guidance as to what the
592 lowest collision energies are at which temperatures in the transition region of the phase diagram can be
593 explored. That is, they will tell us out to what μ_B it will be possible for heavy-ion collisions, anywhere,
594 to study matter in the crossover region and search for a possible critical point.

595 **3.** Heavy-ion collisions at top RHIC energies and at the LHC have now seen several experimental
596 phenomena [85–87] that may be related to the chiral magnetic effect (CME [88, 89], see Sec.3.5.2). In
597 each case, alternative explanations are also being considered [90, 91]. One of the intriguing BES-I results
598 is that the three-particle correlations that are related to charge separation across the reaction plane,

possibly induced by the CME, are robustly observable over most of the BES range but then seem to turn off at $\sqrt{s_{\text{NN}}} = 7.7$ GeV [92], where the elliptic flow v_2 is still robust. This is an indication that v_2 -induced backgrounds alone do not explain the observed correlations. The observation that these three-particle correlations disappear at the lowest energy could prove crucial to understanding their origin and how they are related to the formation of QGP. On the theoretical side, lattice QCD calculations probing the response of the equation of state and transition temperature to the presence of external magnetic fields [93–95], as well as hydrodynamic calculations incorporating magnetic fields and chiral effects, are needed and are being pursued by several groups. On the experimental side, higher statistics BES-II data will make it possible to determine with much greater precision the $\sqrt{s_{\text{NN}}}$ at which this effect turns off and will also make it possible to measure the (related but theoretically more robust) chiral magnetic wave phenomenon [96, 97], which has also been seen at top RHIC energy and at the LHC [98, 99], and which should turn off at the same $\sqrt{s_{\text{NN}}}$ if these interpretations are correct.

4. Theoretical developments over the past decade have identified specific event-by-event fluctuation observables most likely to be enhanced in collisions that cool in the vicinity of the critical point [100, 101]. Higher moments of the event-by-event distribution of the number of protons, or the net proton number, are particularly sensitive [101–103]. STAR has now measured the first four moments (mean, variance, skewness and kurtosis) of the event-by-event distribution of net proton number and net charge at the BES-I energies [77, 104]. At the lowest collision energies, although the statistics are at present rather limiting, there are interesting trends, including e.g. the drop in the kurtosis of the net-proton distribution at $\sqrt{s_{\text{NN}}} = 27$ and 19.6 GeV (see bottom panel in Fig. 5). This drop in and of itself can be at least partially reproduced via prosaic effects captured in model calculations that do not include any critical point. Theoretical calculations of the contributions from critical fluctuations predict [79] that if the freezeout μ_B scans past a critical point as the beam energy is lowered, this kurtosis should first drop below its Poisson baseline and then rise above it. Both the drop and the rise should be largest in central collisions in which the quark-gluon plasma droplet is largest and therefore cools most slowly, allowing more time for critical fluctuations to develop [105]. A recent and still preliminary analysis [78] of the data at $\sqrt{s_{\text{NN}}} = 11.5$ and 7.7 GeV over a larger range in p_T than measured before [77], also shown in the bottom panel of Fig. 5, shows intriguing hints of a rise in the net proton kurtosis in central collisions, but the uncertainties are at present too large to draw conclusions. If this kurtosis does rise at $\sqrt{s_{\text{NN}}}$ values below 19.6 GeV, this would be difficult to understand in conventional terms and thus would be suggestive of a contribution from the fluctuations near a critical point. Determining whether this is so requires the higher statistics that BES-II will provide, as illustrated by the grey band in the bottom panel of Fig. 5.

The present data on moments of both the net proton number and the net charge at the higher BES-I energies are already very useful, as they can be compared to lattice calculations of the Taylor expansions (in μ_B/T) of the baryon number and charge susceptibilities [106]. First versions of this comparison have been reported recently and are being used to provide an independent determination of how the freeze-out values of μ_B and T change with collision energy [107–110]. However, looking ahead, theoretical calculations will need to faithfully account for the dynamical evolution of the medium formed in the collision for a full quantitative exploitation of the experimental data. For the higher statistics BES-II data on the net proton kurtosis, skewness, and other fluctuation observables at low collision energies to determine the location of the critical point on the phase diagram of QCD, if one is discovered, or to reliably exclude its existence within the experimentally accessible region of the phase diagram, a substantial theoretical effort will be needed that couples the sophisticated hydrodynamic calculations referred to above with a fluctuating chiral and dynamically evolving order parameter.

As the following fifth example illustrates, BES-II will also open the door to measurements that were not yet accessible in the first phase of the BES program:

645 **5.** Dileptons are unique penetrating probes with which to study the chiral properties of hot and dense
646 matter. The dielectron invariant mass distributions measured in the BES-I (in data taken at $\sqrt{s_{NN}} = 200,$
647 $62.4, 39$ and 19.6 GeV) have shown that there is a significant enhancement of low mass dileptons below
648 1 GeV relative to a hadronic cocktail [111]. The data so far are qualitatively consistent with a model in
649 which hadron properties are modified in the medium and there is a partonic contribution as well [112].
650 However, data at lower energies with higher statistics are crucial in order to test the predicted strong
651 dependence of dilepton yields on baryon density and draw firm conclusions. The dilepton measurements
652 at and below $\sqrt{s_{NN}} = 19.6$ GeV that BES-II will provide will yield a qualitatively new understanding of the
653 chiral properties of QCD matter with significant baryon density. There are two interesting dilepton mass
654 windows to be studied at BES-II: the low mass window (300 MeV – 700 MeV) and the high mass window
655 (800 MeV – 1.5 GeV). The former will provide indirect information on chiral symmetry restoration via the
656 interaction of vector mesons with (excited) baryons, while the latter will probe chiral restoration directly
657 via the mixing between vector and axial-vector mesons in the hot and dense environment.

658 Each of these five examples makes it clear that in order to maximize the physics outcome from BES-I
659 and BES-II, a coherent effort between experimentalists and theorists working on QCD at nonzero T and
660 μ_B is essential and must be organized and supported. Indeed, there has been considerable progress in
661 lattice QCD recently on the calculation of various QCD susceptibilities [113, 114] and the QCD equation
662 of state in the regime where μ_B is nonzero but sufficiently small compared to $3T_c$ [115, 116]. These
663 lattice calculations provide the necessary inputs for extending to nonzero μ_B the kind of sophisticated
664 hydrodynamic calculations (including initial fluctuations and a late stage hadron cascade) that have been
665 developed over the past few years. For some purposes, these calculations additionally require dynamical
666 coupling to a fluctuating chiral order parameter.

667 In concert, such developments will provide the critical tools for obtaining from BES-I and BES-II data
668 answers to fundamental questions about the phases, the crossover, and perhaps the critical point and
669 first order transition, in the QCD phase diagram. Quantitative understanding of the properties of matter
670 in the crossover region where QGP turns into hadrons will come first. If there is a critical point with
671 $\mu_B < 400$ MeV, BES-II data together with the theoretical tools now being developed should yield
672 quantitative evidence for its presence. The span in T and μ_B that the flexibility of RHIC makes accessible,
673 along with the mentioned technical advantages of measuring fluctuation observables at a collider and
674 recent and planned detector and facility upgrades (e.g. low energy electron cooling), put RHIC in a globally
675 unique position to discover a critical point in the QCD phase diagram if Nature has put this landmark in
676 the experimentally accessible region. Late in the decade, the FAIR facility at GSI will extend this search
677 to even higher μ_B if its collision energies continue to produce matter at the requisite temperatures.

678 **3.3 Probing hot QCD matter at multiple length scales**

679 Hard probes, such as jets and bottomonia, provide the unique opportunity to test the microscopic structure
680 of hot QCD matter at characteristic momentum and length scales. Below we describe the qualitative and
681 quantitative insights into QGP properties these probes have already provided and outline a future program
682 that aims to understand how the QGP properties arise from its microscopic nature.

683 **3.3.1 Jets as microscopic probes of QGP**

684 The properties of jets [117] and their emergence from pQCD have been extensively studied in high-energy
685 physics [118, 119]. One of the earliest discoveries at RHIC was the phenomenon of *jet quenching*, observed
686 as a suppression of high- p_T hadrons and di-hadron correlations in Au+Au collisions [120, 121]. This

687 can be understood as a medium-modification of jet showers [122] through an enhanced rate of gluon
 688 bremsstrahlung, resulting in a depletion of high momentum parton fragmentation products.

689 The virtuality of a hard parton within a jet establishes the intrinsic scale at which it resolves fluctuations
 690 in the medium. As partons cascade down to lower virtualities, they probe the medium over a multitude of
 691 length scales. As long as this resolution scale is much larger than Λ_{QCD} , the parton will be weakly coupled
 692 with the medium and pQCD can be applied to describe its propagation [123–128]. Some partons within a
 693 jet may lose sufficient amounts of energy to encounter non-perturbatively strong coupling [129–132].

694 Jet transport parameters from single-hadron suppression

695 The medium-induced changes to the shower radiation pattern can be described as longitudinal drag/diffusion,
 696 transverse diffusion, and enhanced splitting of the propagating partons. The transport coefficients \hat{q} [133]
 697 and \hat{e} [134] quantify the transverse diffusion and longitudinal drag, respectively.

698 Since the last NP long-range plan, enormous progress has been achieved in the quantitative determination
 699 of \hat{q} and \hat{e} . This has been made possible by new high precision data from RHIC and LHC, as well as
 700 coordinated theory efforts, notably by the JET collaboration. One now obtains a very good description of
 701 the combined RHIC and LHC data on single hadron suppression, as shown in the left panel of Fig. 6.
 702 The extracted values and temperature dependence of the dimensionless ratio \hat{q}/T^3 are plotted in the
 703 right panel of Fig. 6. Using identical initial states and hydro simulations, the JET collaboration has
 704 carried out a systematic analysis of a wide range of pQCD based energy loss schemes [135]. Compared
 705 to earlier studies [136], where the extracted \hat{q} varied by an order of magnitude, the values in the new
 706 analysis [135] differ at most by a factor of 2. This allows for the first time to discern the medium
 707 temperature dependence of \hat{q}/T^3 and demonstrates that quantitative properties of the QGP can be
 708 extracted from jet modification data.

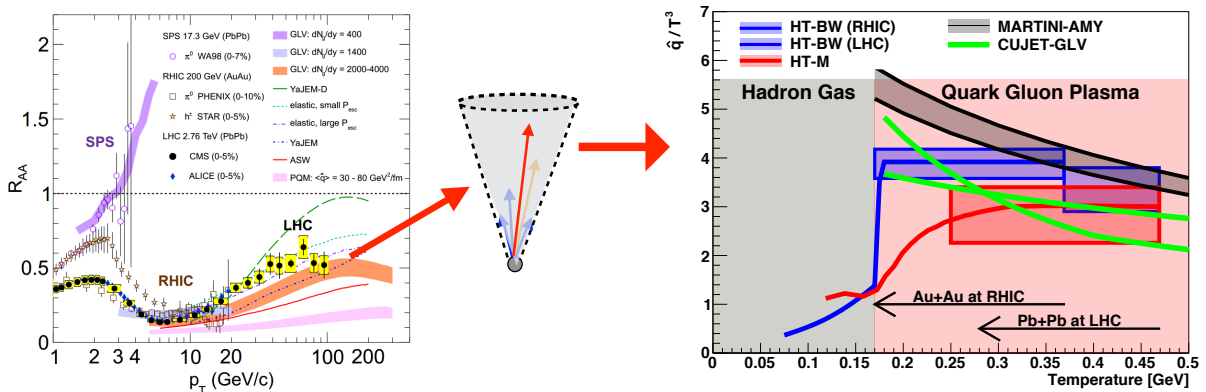


Figure 6: A comparison of several different pQCD based energy loss energy loss schemes to the measured leading hadron suppression in central events at RHIC and LHC, and the extracted scaled (i.e. dimensionless) transport coefficient \hat{q}/T^3 along with its dependence on temperature.

709 Fully reconstructed jets

710 Fully-reconstructed jets have been a crucial tool in high energy physics for precision tests of pQCD [117].
 711 Experimental progress now allows to isolate and reconstruct the entire jet shower from the high-multiplicity
 712 underlying event in heavy-ion collisions. Some of the first LHC heavy-ion results included the observation of
 713 highly asymmetric dijet events, which provided a striking visual demonstration of the energy loss [138, 139].
 714 Since these initial measurements experimental control over the measured jet energies and the understanding

715 of the role of underlying event fluctuations has improved substantially, resulting in precise measurements of
 716 jet suppression and the properties of quenched jets. Photon-jet correlations have been allowed a selection
 717 of the parton kinematics and flavor before energy loss, providing direct evidence for the degradation of
 718 the parton energy as they traverse the medium [140–142].

719 These measurements at the LHC, and pioneering studies at RHIC, have contributed qualitatively new
 720 information on jet modification by the medium. Studies of the cone-size dependence of jet spectra,
 721 jet-hadron correlations and the overall energy flow in dijet events demonstrate that the energy transported
 722 out of the hard core of the jet, as seen in hadron suppression, is not contained within typical jet cone
 723 radii [143,144]. Rather, the energy is recovered in low momentum modes (few GeV or less) at large angles
 724 to the jet direction. The jet structure within the cone reveals only a moderate modification, undergoing a
 725 softening and broadening of the fragmentation pattern.

726 Heavy-quark jets and the mass-dependence of parton energy loss

727 The LHC also allowed new tests of the mass dependence of energy-loss using heavy-quark measurements.
 728 Data on D-meson production and non-prompt J/ψ from B-meson decays (for p_T up to 20 GeV/c) exhibit
 729 the predicted mass hierarchy [145,146], with the heaviest quarks losing significantly less energy than
 730 the lighter flavors. At jet energies of 80 GeV and above, i.e. much higher than the quark mass, tagged
 731 b-quark jets show a similar suppression pattern as inclusive jets.

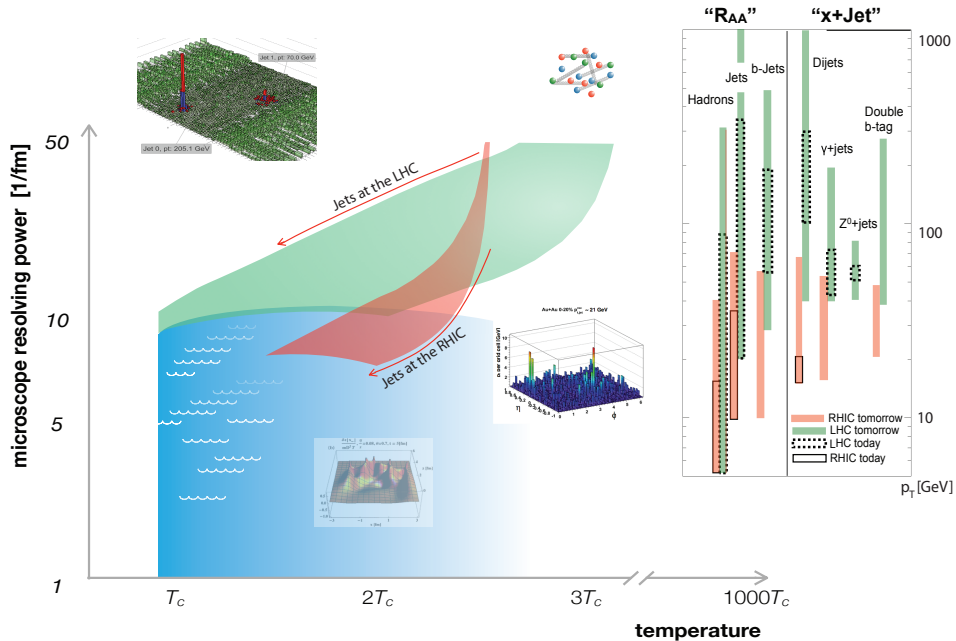


Figure 7: Shown on the left are jet virtuality evolution paths simultaneous with the QGP temperature evolution for central Au+Au and Pb+Pb collisions at RHIC and the LHC. The vertical axis shows the inverse length scale probes in the medium and the blue region where the medium is substantially altering the vacuum parton splitting [137]. This displays the complementarity of RHIC and LHC jet probes in surveying distinct regions of possible QGP excitations and temperature. The right panel shows the momentum regions covered by penetrating probe measurements at RHIC, enabled by high luminosity and the sPHENIX upgrade, and at the LHC with full Run II and Run III statistics.

732 **Future plans – facilities, detectors and measurements**

733 Future jet-based studies built on the achievements at RHIC and LHC will address fundamental questions
 734 about the nature of QGP. These include precise measurements of QGP transport coefficients as a function
 735 of temperature, a detailed characterization of the QGP response to the parton energy loss and studies of
 736 the modification the jets' angular and momentum structure as a function of angular and momentum scale.
 737 In combination, the goal of these studies is to understand the microscopic (or quasi-particle) nature of
 738 QGP at varying scales, and to understand how the macroscopic QGP liquid emerges from the underlying
 739 QCD degrees of freedom. A schematic sketch of the present and expected future resolving power for the
 740 structure of QCD matter at different temperatures in RHIC and LHC experiments is shown in Fig. 7 [137].

741 This program will be enabled by the evolution of the RHIC and LHC accelerator facilities, upgrades to
 742 the existing experiments and the construction of a state-of-the-art jet detector at RHIC, sPHENIX [137].
 743 In parallel, the recently emerged experiment/theory collaborations will be strengthened and expanded, to
 744 fully utilize the increased precision and range of experimental observables.

745 **At BNL** the RHIC science mission will be completed with three planned heavy-ion running campaigns as
 746 shown in Fig. 8 (left). A key goal of the 2014-16 period is to measure heavy flavor probes of the QGP
 747 using the newly installed silicon vertexing detectors in PHENIX and STAR. For 2018-19, Phase II of the
 748 RHIC Beam Energy Scan program (BES-II) is foreseen. In 2021-22, precision jet quenching and quarkonia
 749 measurements will be made possible by the installation of sPHENIX.

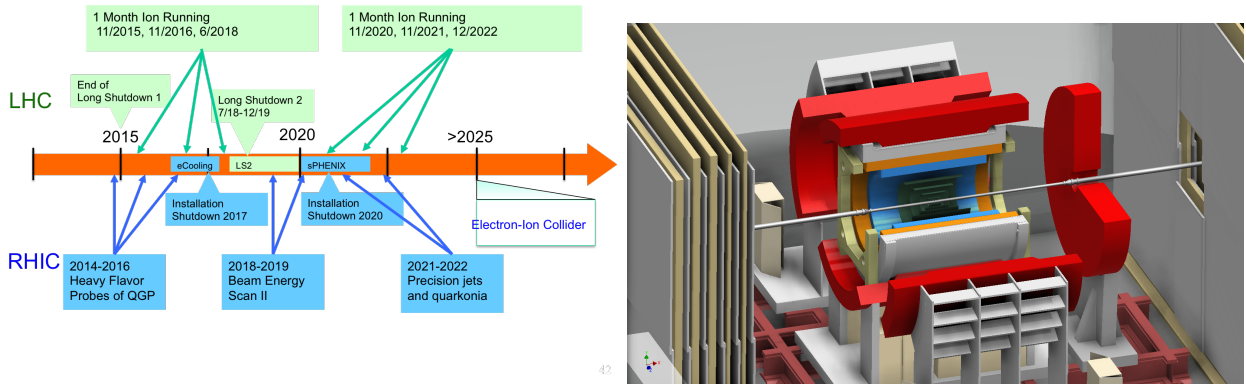


Figure 8: (Left) The timeline for future RHIC and LHC heavy-ion running. (Right) A cut-away view of the proposed sPHENIX upgrade to the PHENIX experiment, showing the inner tracking system, the electromagnetic calorimeter, the BaBar solenoid and the hadronic calorimeter.

750 The proposed sPHENIX detector, shown in the right panel of Fig. 8, would dramatically extend the
 751 range of jets measurable at RHIC, as well as provide precision spectroscopy of quarkonia, in particular
 752 the upsilon states. The program relies on a very high data acquisition bandwidth, which combined with
 753 RHIC II luminosities enables the measurements of jet energies up to 70 GeV. The sPHENIX design takes
 754 advantage of various technological advances to minimize costs. sPHENIX also provides one route for a
 755 for a smooth evolution to a full-capability EIC detector.

756 **The LHC** is now preparing for Run II, foreseen to include p+p, p+Pb and heavy-ion data taking from
 757 2015 to 2018. Run II will be followed by a shutdown from 2018 to 2020 (LS2) and Run III from 2020 to
 758 2023. For both the p+p and Pb+Pb data taking, the LHC upgrades during the current shutdown should
 759 allow for collisions at close to the design energy, i.e., about 5 TeV per nucleon pair for Pb+Pb. Collision
 760 rates are expected to exceed the design values by up to one order of magnitude, with a combined Run II
 761 and III goal to deliver about 10 nb⁻¹ per experiment. In combination, the increased collision energy and

762 luminosity will increase statistics for high p_T probes by about a factor of 200.

763 To exploit this improved accelerator performance, ALICE, ATLAS and CMS are undergoing significant
764 upgrades during the current shutdown and LS2. For ATLAS and CMS, these upgrades are mostly driven
765 by the needs of the p+p program. Of particular importance for future heavy-ion running are upgrades to
766 the inner tracker detectors, extending the reach of charged particle measurements, and upgrades to the
767 trigger systems, allowing the experiments to fully sample the expected collision data for hard probes.

768 ALICE is preparing for Run II with an expansion of the calorimetric coverage (EMCAL) which will allow
769 for dijet studies and improved jet triggering. During LS2 the experiment's data taking capabilities will be
770 significantly enhanced with major upgrades to detector readout and data acquisition systems. In addition a
771 new silicon inner tracker will be installed. While precision measurements of low p_T open heavy flavor are
772 the main physics driver for these upgrades, they also benefit the intermediate and high p_T jet quenching
773 program.

774 These RHIC and LHC facility and experiment upgrades benefit jet physics studies in three major ways.
775 The statistical precision and kinematic reach for commonly used jet physics observables is vastly increased.
776 For single charged hadrons and reconstructed jets, the p_T reach will be extended by a factor of 2–3, up
777 to 40 GeV for hadrons and 70 GeV for jets at RHIC and 300 GeV and 1 TeV, respectively, at the LHC.
778 This will further improve the precision of the extraction of e.g. \hat{q} and its temperature dependence from
779 model comparisons.

780 A second benefit is improved access to rare, highly specific observables, such as isolated photon + jet
781 correlations at RHIC and LHC, as well as Z^0 +jet correlations at the LHC. For example, LHC experiments
782 will record more than 5×10^5 photons with $p_T^\gamma > 60$ GeV, compared to about 3000 in the Run I data sets.

783 Finally, the very high statistics jet samples enable the measurement of a new generation of jet shape
784 observables. There is intense activity in developing generalized jet structure variables for the pp program
785 at the LHC to maximize the efficiency of discovery measurements by improving quark/gluon discrimination
786 and the tagging of boosted objects. Heavy-ion studies of the modification of the jet momentum and
787 angular structure through medium interactions will benefit greatly from these developments.

788 **Jet physics outlook**

789 In combination, these developments will enable a coherent RHIC and LHC physics program employing
790 well-calibrated common observables. As shown in Fig. 7, future RHIC and LHC measurements will both
791 overlap with and complement each other. This program will have three main components:

792 First, a combined global analysis of RHIC and LHC data will allow a precise determination of the values
793 and temperature dependence of QGP transport coefficients. Both the RHIC and LHC final states represent
794 an integral of jet-medium interactions over the evolution of both jet and medium from initial to final state.
795 To disentangle the temperature dependence from this evolution it will be essential to deploy directly
796 comparable observables (theoretically and experimentally) in different QGP temperature regimes, with
797 particular focus on the fraction of their evolution spent in vicinity to the phase transition region that will
798 be passed by all collisions.

799 The second component relies on the increased systematic and statistical precision afforded by new probes
800 (e.g. photon-jet) to identify the medium response to the modified jet radiation and further elucidate the
801 liquid nature of the medium in its response to local perturbations.

802 Third, precision measurements of the angular and momentum structure of jets can be used to characterize
803 the microscopic structure of the QGP, using hard partons as probes in “Rutherford scattering” off effective
804 QGP constituents or quasi-particles. Studies include potential modifications to the back-to-back jet
805 scattering distributions, as well as modifications of the intra-jet angular structure. For the latter, the

806 correlated angular and momentum evolution of the jet from the initial scattering to the final hadronic
807 structure probes a wide range of scales, opening a window to interactions of jet and QGP constituents
808 between vacuum-like and in-medium cascade regimes. To elucidate the physics of this intermediate
809 window, a systematic variation of both the jet conditions and medium conditions and dynamics is
810 necessary. Combining RHIC and LHC measurements will allow control over initial density and temperature
811 (in particular in respect to their vicinity to the critical temperature) and expansion dynamics of the
812 system. The different energy regimes and tagging of particular initial states (photon+jet, b-tagged jets,
813 multi-jet events) will allow selection of different or common jet populations in relation to different medium
814 conditions. Success in this long-term endeavor will require a global analysis of a diverse set of RHIC and
815 LHC data in an improved, well controlled theoretical framework matched to the experimental observables.

816 **3.3.2 Probing the QGP with bottomonia**

817 A key probe of the strength and nature of the color interactions in the QGP are precision measurements
818 of bottomonia states. The three lowest bound states of $b\bar{b}$ (Υ 1s, 2s, 3s) have a range of binding energies
819 and length scales that allow one to understand the temperature dependence of plasma screening [147]
820 that leads to a characteristic sequential suppression pattern [148] for in-medium quarkonium bound states.
821 Compared to charmonia, bottomonia have the advantage that, because of the rarity of b quarks even
822 at LHC energies, contributions from $b\bar{b}$ recombination at the end of the life of the quark-gluon plasma,
823 that would dilute the suppression signal caused by color screening, can be neglected. The theoretical
824 interpretation of any observed medium modification of bottomonium production yields is therefore much
825 less affected by model uncertainties than for charmonia [149].

826 First detailed bottomonium measurements at the LHC from CMS show the expected ordering by their
827 size and binding energies in the suppression of these states as a function of collision centrality [150]. First
828 measurements at RHIC without resolving the three states have also been completed [151, 152]. Critical
829 to the effort to understand the screening interactions as a function of temperature are simultaneous
830 precision measurements at RHIC and the LHC (probing cooler and hotter plasmas) in p+p, p+A, and
831 A+A, with sufficient statistics to map out the centrality and p_T dependencies. Increased luminosities at
832 the LHC in Run II and Run III will provide these data. At RHIC, additional statistics will be provided by
833 the STAR MTD upgrade; ultimately, for matched precision at RHIC and the LHC, the sPHENIX upgrade
834 is required.

835 **3.4 A polarized p+A program for initial-state and low-x phenomena**

836 Four dominant questions have been identified that can be explored in a polarized p+p and p+A program:
837 1) What is the nature of the spin of the proton? 2) How do quarks and gluons hadronize into final-state
838 particles? 3) How can we describe the multidimensional landscape of nucleons and nuclei? 4) What is
839 the nature of the initial state in nuclear collisions? The first question is discussed in the “cold QCD”
840 Town Meeting summary and associated white papers. The remaining questions share particularly strong
841 synergies with the goals of the hot QCD community and are discussed below.

842 At the high collision energies of RHIC and the LHC, the available phase space for radiating small- x
843 gluons and quark-antiquark pairs is very large. Since each emitted parton is itself a source of additional
844 gluons, an exponentially growing cascade of radiation is created which would eventually violate unitarity.
845 However, when the density of partons in the transverse plane becomes large enough, softer partons
846 begin to recombine into harder ones and the gluon density saturates. This limits the growth of the
847 cascade and preserves the unitarity of the S -matrix. The transverse momentum scale below which these

848 nonlinear interactions dominate is known as the *saturation scale* Q_s . The saturation scale grows with
849 energy, but also with the size of the nucleus as $Q_s^2 \sim A^{1/3}$. For high enough energies Q_s is large and the
850 corresponding QCD coupling is weak: $\alpha_s(Q_s) \ll 1$. This makes it possible to calculate even bulk particle
851 production using weak coupling methods, although the calculation is still nonperturbative due to the large
852 field strengths. Because the gluonic states have large occupation numbers, the fields behave classically.
853 The classical field theory describing the saturation domain is known as the “Color Glass Condensate”
854 (CGC) [153].

855 The ideal probe of the CGC description are dilute-dense collisions, where a simple small projectile
856 collides with a large nucleus. At RHIC and the LHC this makes proton-nucleus collisions important for
857 understanding saturation. Significant progress has been made in describing the systematics of particle
858 production as a function of transverse momentum and rapidity in proton-proton and proton-nucleus
859 collisions with CGC calculations, which match the collinearly factorized perturbative QCD description at
860 high transverse momenta. The case of saturation effects in multiparticle correlations as a function of
861 azimuthal angle and rapidity remains more open. While there are contributions to these correlations that
862 originate already in the nuclear wave functions [154], experimental evidence points to strong collective
863 behavior also in the final state of proton-nucleus and even proton-proton collisions. The versatility of
864 RHIC to systematically change the size of the projectile nucleus and complement p+A with d+A, $^3\text{He}+A$
865 etc. collisions over a wide range of collision energies is unparalleled and a key to exploring where these
866 collective effects turn on. Precise and controlled access to the high energy nucleus can be used to
867 disentangle the effects of strong collectivity in the initial wave functions and the final state.

868 As noted elsewhere, an EIC [1] which can measure the transverse and longitudinal structure of the small- x
869 gluons in nuclei is crucial for a deep understanding of hadron wave functions. However, measurements
870 of forward photon, J/ψ , Drell-Yan, inclusive and di-jet, and hadron/jet correlation probes in p+A
871 collisions [155, 156] provide a unique opportunity to make timely progress in our understanding and to
872 complement the eventual EIC measurements. In particular, the observables mentioned are related to
873 different transverse momentum dependent gluon distributions (TMDs) that have previously been studied
874 at higher x . Recent theoretical advances [157] have clarified the relation of these distributions to each
875 other via the CGC picture, in both p+A and e+A collisions, and they are opening up new exciting
876 connections to polarized observables. One particular example of these connections is the possibility of
877 extracting the saturation scale Q_s in nuclei by comparing transverse single spin asymmetries measured in
878 polarized p+p and polarized p+A collisions, for different nuclei and at different beam energies [158, 159].
879 Another exciting opportunity in polarized p+A collisions is the possibility of extracting generalized parton
880 distributions (GPDs) for gluons. This can be achieved for instance in exclusive J/Ψ production via
881 photon-gluon fusion of quasi-real ultraperipheral photons from the nucleus with gluons from the polarized
882 proton [160].

883 The study of these novel TMDs and GPDs will deepen our understanding of the momentum and spatial
884 structure of polarized and unpolarized quarks and gluons in hadrons. These studies require as key
885 ingredients establishing factorization and universality that help separate the structure of the hadron wave
886 function from the dynamics of the probe. From this perspective, even if measurements at a future EIC
887 with an electron probe provides unmatched precision, a polarized proton-nucleus program provides a
888 complementarity that may prove essential.

889 From another perspective, proton-nucleus collisions provide crucial consistency checks for our understanding
890 of heavy-ion collisions: Clearly, theoretical descriptions developed for partonic interactions in a hot and
891 dense QCD medium must also be consistent with the effects of the cold QCD medium on hadronization
892 of a colored probe that can be studied in p+A collisions. Such collisions, across a range of beam energies
893 and target species, will therefore provide important control experiments for our theoretical understanding

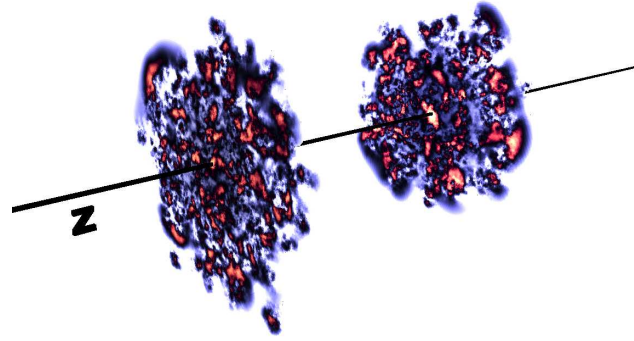


Figure 9: Color fields of the two nuclei before the collision, from [161]

894 of jet quenching in heavy-ion collisions, on a time scale that precedes the construction of an EIC.

895 The theoretical description of the initial stage of quark gluon plasma formation has become increasingly
 896 detailed. State of the art calculations [24, 162] now combine a fluctuating nuclear geometry with a
 897 microscopic QCD description of the dynamics of matter formation (see Fig. 9), going beyond the Glauber
 898 model descriptions of the geometry. As discussed in Sec. 3.1, these initial-state calculations, combined
 899 with detailed measurements of correlations and fluctuations in the observed flow patterns have helped
 900 to significantly improve the precision of the first quantitative experimental determinations of e.g. the
 901 viscosity/entropy ratio η/s . Further, as noted, proton-nucleus collisions have also provided surprises in
 902 their own right—we now understand the resolution of these to be sensitive to the detailed spatial structure
 903 of partons in both protons and heavier nuclei. The importance of a polarized p+A program is therefore
 904 two-fold: (i) It will provide unique and essential information on the parton structure of proton and nuclear
 905 wave functions. (ii) The implementation of this information in models of heavy-ion collision will provide
 906 more sensitive tests of and precise extraction of the parameters of the Little Bang Standard Model.

907 **3.5 Opportunities and challenges in theory**

908 **3.5.1 Progress since the 2007 Nuclear Physics Long Range Plan**

909 Part of Recommendation IV of the 2007 Long Range Plan was the appreciation that *“achieving a*
 910 *quantitative understanding of the properties of the quark-gluon plasma also requires new investments*
 911 *in modeling of heavy-ion collisions, in analytical approaches, and in large-scale computing.”* Since then
 912 there has been tremendous progress along these lines. Convergence has been reached in lattice QCD
 913 calculations of the temperature for the crossover transition in strongly interacting matter which has now
 914 been established at $145 \text{ MeV} < T_c < 163 \text{ MeV}$ [32, 63, 64, 163]. Continuum extrapolated results for the
 915 equation of state, the speed of sound and many other properties of strong interaction matter have also
 916 been provided [31, 32]. The modeling of the space-time evolution of heavy-ion collisions has become
 917 increasingly reliable. (2+1)-dimensional, and subsequently, (3+1)-dimensional relativistic viscous fluid
 918 dynamics computations have been performed. All such computations use an equation of state extracted
 919 from lattice QCD. A paradigm shift occurred with the broad appreciation of the importance of fluctuations.
 920 For heavy-ion collisions at the highest RHIC and at LHC energies, the Color Glass Condensate (CGC)
 921 effective theory of QCD provides a framework to compute the properties of the fluctuating initial state.
 922 Under the aegis of the JET topical collaboration, a successful effort was undertaken to consolidate the

923 results of different approaches to computing the transport properties of jets as they traverse the strongly
924 correlated quark-gluon plasma. Much progress has been made towards a systematic understanding from
925 first principles of the properties of strongly interacting matter at non-zero baryon number density. Such
926 studies rely heavily on the development of theoretical concepts on critical behavior signaled by conserved
927 charge fluctuation [65, 79, 102]. They are accessible to lattice QCD calculations which opens up the
928 possibility, via dynamical modeling, for a systematic comparison of experimental fluctuation observables
929 with calculations performed in QCD [106–110]. This will greatly profit from the steady development of
930 computational facilities which are soon expected to deliver sustained petaflop/s performance for lattice
931 QCD calculations.

932 An outcome of these efforts has been the development of a standard dynamical framework for heavy-ion
933 collisions, as described Sec. 3.1. Relativistic viscous fluid dynamics forms the core of this dynamical
934 framework and, at high RHIC and LHC energies, it describes the largest part of the evolution history of the
935 Little Bang – the explosive expansion of the hot and dense QCD medium formed in the collisions. Much
936 recent theoretical work has led to increasingly complete formulations of this theory and improved our
937 understanding of its limits of applicability to heavy-ion collisions, and further improvements to optimize
938 the framework for such applications are ongoing.

939 As described earlier in Sec. 3.1, this standard framework does a good job of describing the wealth of data
940 obtained on bulk spectra and event-by-event distributions of anisotropy coefficients, both at RHIC and the
941 LHC. To turn this framework into a Little Bang Standard Model requires fixing all the model parameters
942 that cannot (yet) be directly computed theoretically, and further refining our descriptions of the initial
943 energy deposition and thermalization stages and the interfaces between the different collision stages (see
944 following subsection). This process has started but is by no means complete. Finalizing the Little Bang
945 Standard Model also requires new sophisticated model/data comparison tools and technologies that are
946 just now being developed. Still, with the limited data/theory comparison tools that have so far been
947 brought to bear on the large sets of experimental data collected at RHIC and LHC, the specific shear
948 viscosity η/s of QCD matter created at RHIC could be constrained to be approximately 50% larger than
949 the conjectured lower bound of $1/4\pi = 0.08$, and to be about 2.5 times larger than this bound at the
950 LHC.

951 Concurrent efforts on extracting the jet quenching parameter \hat{q}/T^3 from similar theory-data comparisons
952 have narrowed the range of values for this parameter to $2 < \hat{q}/T^3 < 6$ within the temperature range probed
953 by RHIC and the LHC, nearly an order of magnitude lower than some previous estimates for this quantity.

954 **3.5.2 Open questions and future goals**

955 The development of a broad consensus on the elements of a Standard Model paradigm provides the
956 basis for a deeper exploration of each of these elements, as well as the opportunity to further solidify
957 the overall picture. Some of the challenging issues over which we need to get better control include i)
958 the pre-equilibrium “Glasma” dynamics of coherent gluon fields, and the approach to thermalization;
959 ii) the extraction of the values and temperature dependences of transport parameters that reflect the
960 many-body QCD dynamics in deconfined matter; iii) the initial conditions at lower collision energies where
961 the Glasma framework breaks down; iv) the proper inclusion of the physics of hydrodynamic fluctuations;
962 v) an improved treatment of hadron freeze-out and the transition from hydrodynamics to transport theory,
963 in particular the treatment of viscous corrections that can influence the extraction from data of the
964 physics during the earlier collision stages.

965 Quantitative improvements in these aspects of the dynamical modeling of a heavy-ion collision will lead to
966 increased precision in the extraction of the underlying many-body QCD physics that governs the various

967 collision stages. Additional conceptual advances in our understanding of QCD in matter at extreme
968 temperatures and densities are required to answer a number of further outstanding questions. We here
969 list a few of them, in chronological order as seen by an observer inside a heavy-ion collision:

970 **1.** A complete quantitative understanding of the properties of the nuclear wave functions that are
971 resolved in nucleus-nucleus and proton-nucleus collisions so far remains elusive. Progress requires the
972 extension of computations of the energy evolution of these wave functions in the Color Glass Condensate
973 (CGC) framework to next-to-leading logarithmic accuracy, and matching these to next-to-leading order
974 perturbative QCD computations at large momenta. Simultaneously, conceptual questions regarding the
975 factorization and universality of distributions need to be addressed for quantitative progress. These ideas
976 will be tested in upcoming proton-nucleus collisions at RHIC and the LHC, and with high precision at a
977 future EIC.

978 **2.** How the Glasma thermalizes to the quark-gluon plasma is not well understood. There has been
979 significant progress in employing classical statistical methods and kinetic theory to the early stage dynamics
980 – however, these rely on extrapolations of weak coupling dynamics to realistically strong couplings.
981 Significant insight is also provided from extrapolations in the other direction – to large couplings – using
982 the holographic AdS/CFT correspondence between strongly coupled $\mathcal{N} = 4$ supersymmetric Yang-Mills
983 theory in four dimensions and weakly coupled gravity in an $\text{AdS}_5 \times S_5$ space. Significant numerical and
984 analytical progress can be anticipated in this fast evolving field of non-equilibrium non-Abelian plasmas.

985 **3.** A novel development in recent years has been the theoretical study of the possible role of quantum
986 anomalies in heavy-ion collisions. A particular example is the Chiral Magnetic Effect (CME), which
987 explores the phenomenological consequences of topological transitions in the large magnetic fields created
988 at early times in heavy-ion collisions. How the sphaleron transitions that generate topological charge
989 occur out of equilibrium is an outstanding question that can be addressed by both weak coupling and
990 holographic methods. Further, the effects of these charges can be propagated to late times via anomalous
991 hydrodynamics. While there have been hints of the CME in experiments, conventional explanations
992 of these exist as well. For a future beam energy scan, quantifying the predictions regarding signatures
993 of quantum anomalies is crucial. This requires inclusion of the anomalies into the standard dynamical
994 framework. We note that the study of the CME has strong cross-disciplinary appeal, with applications in
995 a number of strongly correlated condensed matter systems.

996 **4.** Noteworthy progress has been made in thermal field theory computations of photon and di-lepton
997 production in heavy-ion collisions, where NLO computations are now available. A challenging problem is
998 to find clear signatures of chiral symmetry restoration that are separable from the underlying resonance
999 background. Discrepancies between theory and experiment, for example the “photon v_2 puzzle” mentioned
1000 in Sec. 3.1, point to missing physics, with several unconventional explanations ranging from transient
1001 Bose-Einstein Condensates to effects arising from the coupling of the conformal anomaly to external
1002 magnetic fields.

1003 **5.** As observed in Sec. 3.3.1, progress has been made in quantifying the jet quenching parameter \hat{q} ,
1004 which characterizes an important feature of the transverse response of the quark-gluon medium. However,
1005 significant challenges persist. Another important transport parameter \hat{e} , characterizing the longitudinal
1006 drag of the medium on the hard probe, also needs to be quantified. Much recent theoretical effort
1007 has gone into extending the splitting kernel for gluon radiation by a hard parton traversing a dense
1008 medium to next-to-leading-order accuracy. In this context Soft Collinear Effective Theory (SCET),
1009 imported from particle theory, has proven a promising theoretical tool whose potential needs to be further
1010 explored. There have been recent theoretical developments in understanding how parton showers develop
1011 in the quark-gluon medium; confronting these with the available jet fragmentation data requires their
1012 implementation in Monte-Carlo codes coupled to a dynamically evolving medium. There have been recent

1013 attempts to compute the jet quenching parameter using lattice techniques; while very challenging, such
1014 studies provide a novel direction to extract information on the non-perturbative dynamics of the strongly
1015 correlated quark-gluon plasma.

1016 **6.** Quarkonia and heavy flavor, like jets, are hard probes that provide essential information on the
1017 quark-gluon plasma on varied length scales. Further, the two probes find common ground in studies
1018 of b-tagged and c-tagged jets. In proton-proton and proton-nucleus collisions, non-relativistic-QCD
1019 (NRQCD) computations are now standard, and these have been extended to nucleus-nucleus collisions,
1020 even to next-to-leading order accuracy. Lattice studies extracting quarkonium and heavy-light meson
1021 spectral functions have increased in sophistication, and clear predictions for the sequential melting of
1022 quarkonium states exist and need to be confronted with experiment. The direct connection to experiment
1023 requires, however, considerable dynamical modeling effort.

1024 **7.** An outstanding intellectual challenge in the field is to map out the QCD phase diagram. While the
1025 lattice offers an *ab initio* approach, its successful implementation is beset by the well known sign problem,
1026 which is also experienced in other branches of physics. Nonetheless, approaches employing reweighting
1027 and Taylor expansion techniques have become more advanced and are now able to explore the equation of
1028 state and freeze-out conditions at baryon chemical potentials $\mu_B/T \leq 2$. This covers a large part of the
1029 energy range currently explored in the beam energy scan and suggests that a possible critical endpoint
1030 may only be found at beam energies less than 20 GeV. Other promising approaches include the complex
1031 Langevin approach [164, 165] and the integration over a Lefschetz thimble [166, 167]. There has been
1032 considerable work outlining the phenomenological consequences of a critical point in the phase diagram.
1033 However, quantitative modeling of how critical fluctuations affect the measured values of the relevant
1034 observables will require the concerted theoretical effort sketched in Sec. 3.2.

1035 We cannot emphasize strongly enough that the impressive intellectual achievements outlined and the
1036 challenges ahead depend strongly on further development of the theory of strongly interacting matter
1037 which involves advances in heavy ion phenomenology, perturbative QCD, lattice QCD and effective field
1038 theories for QCD as well as the strong synergy with overlapping and related areas in particle physics,
1039 condensed matter physics, cold atom physics, string theory and studies of complex dynamical systems. In
1040 the case of string theory and condensed matter physics, a strong argument can be made that developments
1041 in heavy-ion collision theory have influenced developments in those fields. The depth and extent of
1042 interaction of this sub-field of nuclear theory with other branches of physics is perhaps unprecedented in
1043 nuclear physics.

1044 **3.5.3 What the field needs**

1045 Looking ahead, sustaining and expanding the health of this sub-field of nuclear theory will depend on the
1046 following key items:

1047 **1.** Strong continued support of the core nuclear theory program supporting university PI's, national lab
1048 groups and the National Institute for Nuclear Theory (INT). Together, they play an essential role in
1049 generating and implementing key ideas driving the field, and in training the next generation of students
1050 and post-doctoral fellows.

1051 **2.** Strong continued support of the DOE Early Career Award (ECA) program in Nuclear Theory, as well as
1052 the NSF Early Career Development (CAREER) and Presidential Early Career (PECASE) award programs.
1053 These provide an important opportunity for the field to recognize and promote the careers of the most
1054 outstanding young nuclear theorists.

- 1055 **3.** Strong support of expanded computational efforts in nuclear physics, as outlined in the Computational
1056 Nuclear Physics white paper and reflected in Recommendation #3 of this document (see Section 2).
1057 Progress in heavy-ion theory is strongly linked to the availability of a diverse and expanding array of
1058 computational resources, including both leadership class and capacity class computational resources.
- 1059 **4.** Continuation and expansion of Topical Research Collaboration program. These collaborations are
1060 especially valuable where there are several strains of theory developments that need to be coordinated
1061 and harnessed to address specific goals. An example of such a successful effort is the JET Topical
1062 Collaboration involving the co-ordinated effort of both theorists and experimentalists, as discussed earlier
1063 in this document. The field has several outstanding challenges that require the synthesis of a broad range
1064 of expertise, and it could strongly benefit from an expansion of such collaborations.
- 1065 **5.** Strong support for the conclusions of the Education and Innovation Town Hall meeting. The numbers
1066 of scientists from underrepresented minorities and women are particularly low in nuclear theory. We
1067 encourage efforts to remedy this situation to a level that at least reflects the diversity of talent seen in
1068 other fields of science.

1069 4 Understanding the glue that binds us all: The Electron Ion Collider

1070 4.1 The next QCD frontier

1071 Atomic nuclei are built from protons and neutrons, which themselves are composed of quarks that are
1072 bound together by gluons. Quantum Chromo-Dynamics (QCD), the gauge theory of the strong interaction,
1073 not only determines the structure of hadrons but also provides the fundamental framework to understand
1074 the properties and structure of atomic nuclei at all energy scales in the universe. QCD is based on the
1075 exchange of massless gauge bosons called gluons between the constituents of hadrons, quarks. Without
1076 gluons there would be no protons, no neutrons, and no atomic nuclei. Matter as we know it would
1077 not exist. Understanding the interior structure and interactions of nucleons and nuclei in terms of the
1078 properties and dynamics of the quarks and gluons as dictated by QCD is thus a fundamental and central
1079 goal of modern nuclear physics.

1080 Gluons do not carry an electric charge and are thus not directly visible to electrons, photons, and other
1081 common probes of the structure of matter. An understanding of their role in forming the visible matter in
1082 the universe thus remains elusive. The Electron Ion Collider (EIC) with its unique capability to collide
1083 polarized electrons with polarized protons and light ions at unprecedented luminosity, and with heavy
1084 nuclei at high energy, will be the first precision microscope able to explore how gluons bind quarks to
1085 form protons and heavier atomic nuclei.

1086 By precisely imaging gluons and sea quarks inside the proton and nuclei, the EIC will address some of the
1087 deepest fundamental and puzzling questions nuclear physicists ask:

- 1088 • Where are the gluons and sea quarks, and how are their spins, distributed in space and momentum
1089 inside the nucleon? What is the role of the orbital motion of sea quarks and gluons in building the
1090 nucleon spin?
- 1091 • What happens to the gluon density in nuclei at high energy? Does it saturate? Does this mechanism
1092 give rise to a universal component of matter in all nuclei, even the proton, when viewed at close to
1093 the speed of light?
- 1094 • How does the nuclear environment affect the distributions of quarks and gluons and their interactions
1095 in nuclei? How does nuclear matter respond to a fast moving color charge passing through it? How
1096 do quarks dress themselves to become hadrons?

1097 A full understanding of QCD, in a regime relevant to the structure and properties of hadrons and nuclei,
1098 demands a new era at the EIC of precision measurements that can probe them in their full complexity.
1099 Theoretical advances over the past decade have resulted in the development of a powerful formalism that
1100 provides quantitative links between such measurements and the above questions physicists are trying
1101 to answer. A second important advance in recent years is the increasing precision and reach of *ab*
1102 *initio* calculations performed with lattice QCD techniques. Using the experimental data from an EIC,
1103 physicists will, for the first time, be able to undertake the detailed comparative study between experimental
1104 measurements and the predictions made by continuum- and lattice-QCD theory, as well as elucidate
1105 aspects of the structure of hadrons and nuclei whose investigation still requires more phenomenological
1106 theoretical methods.

1107 The experimental study of how hadrons and nuclei emerge from the laws of QCD is a global scientific
1108 priority. Two world-leading facilities in the U.S., CEBAF at Jefferson Lab and RHIC at BNL, are
1109 international centers for the study of QCD. With the increase of its beam energy to 12 GeV, Jefferson Lab
1110 will soon operate a unique electron microscope, which will systematically map the structure of protons
1111 and other nuclei in the valence quark region. In addition to its discovery and continuing exploration of the

1112 strongly coupled quark gluon plasma (QGP), RHIC has used its unique capability as a polarized proton
 1113 collider to make a first direct determination of the contribution of the gluons to the proton's spin.

1114 The high energy, high luminosity polarized EIC will unite and extend the current scientific programs
 1115 at CEBAF and RHIC in dramatic and fundamentally important ways. It will enable us to image the
 1116 transverse momentum and position distributions of quarks and gluons inside fast moving hadrons. When
 1117 hadrons move at nearly the speed of light, the low-momentum gluons contained in their wave functions
 1118 become experimentally accessible. The EIC will study the way in which gluons interact with each other
 1119 by splitting and fusing in addition to providing three-dimensional images of the confined motion of quarks
 1120 and gluons and their spatial distribution. By colliding electrons with heavy nuclei moving with the light
 1121 speed, the EIC will provide access to a so far unconfirmed regime of matter where abundant gluons
 1122 dominate its behavior. Such universal cold gluon matter is an emergent phenomenon of QCD dynamics
 1123 and of high scientific interest and curiosity. Furthermore, its properties and its underlying QCD dynamics
 1124 are critically important for understanding the dynamical origin of the creation of the QGP from colliding
 1125 two relativistic heavy ions, and the QGPs almost perfect liquid behavior. Enabling these research activities
 1126 all in one place, the EIC will be a true "QCD Laboratory", unique of its kind in the world.

1127 4.2 Science highlights and deliverables at the EIC

1128 The high energy, high luminosity polarized EIC will unite and extend the scientific programs at CEBAF,
 1129 RHIC and the LHC in dramatic and fundamentally important ways.

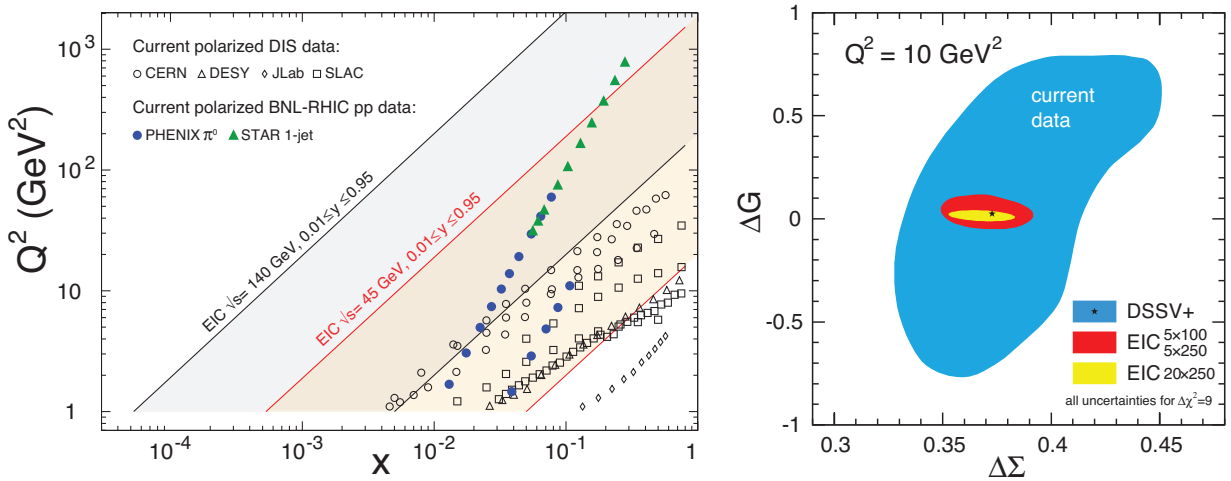


Figure 10: **Left panel:** The increase in the proton momentum fraction x vs. the square of the momentum transferred by the electron to proton, Q^2 , accessible to the EIC in e+p collisions. **Right panel:** The projected reduction in the uncertainties of the gluons' (ΔG) and quarks' ($\Delta \Sigma$) contributions to the proton's spin.

1130 **Proton Spin:** Recent measurements at RHIC along with state-of-the-art perturbative QCD analyses
 1131 have shown that gluons carry approximately 20-30% of the proton's helicity, similar to the contribution
 1132 from quarks and anti-quarks. The blue band in the right panel of Figure 10 shows the current level of
 1133 uncertainties. The knowledge is limited by the x -range explored so far. The EIC would greatly increase
 1134 the kinematic coverage in x and Q^2 , as shown in the left panel of Figure 10, and hence reduce this
 1135 uncertainty dramatically, to the level depicted by the red and yellow bands in the right panel.

1136 **Motion of quarks and gluons in a proton:** Semi-inclusive measurements with polarized proton beams
 1137 would enable us to selectively and precisely probe the correlations between the spin of a fast moving
 1138 proton and the confined transverse motion of both the quarks and gluons within it. Images in momentum
 1139 space as shown in the left panel of Figure 11 are simply unattainable without the polarized electron and
 1140 proton beams of the proposed EIC.

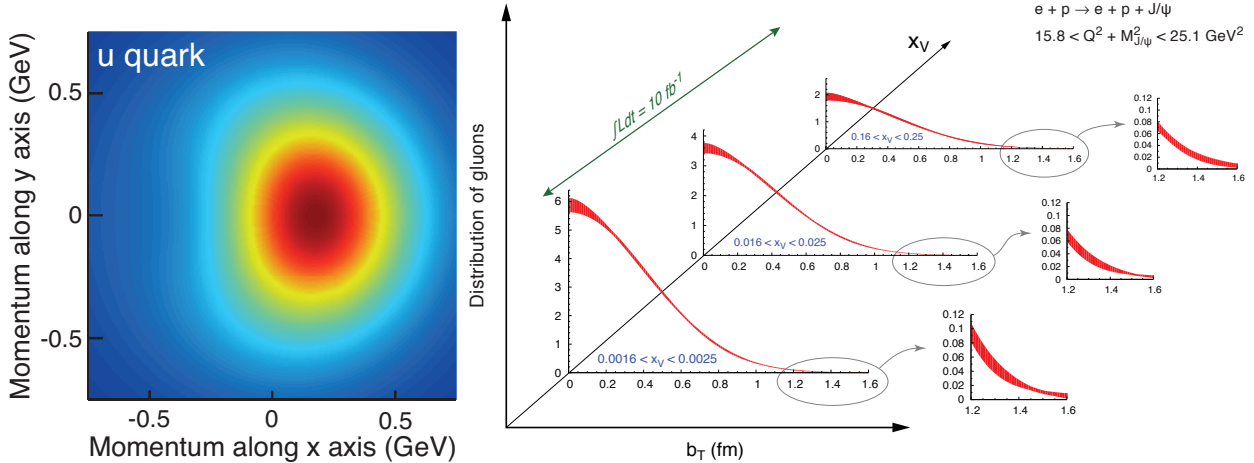


Figure 11: **Left panel:** Transverse momentum distribution of a sea u -quark with longitudinal momentum fraction $x = 0.1$ in a transversely polarized proton moving in the z -direction, while polarized in y -direction. The color code indicates the probability of finding the up quarks, with dark red indicating the highest probability. **Right panel:** Projected precision of the transverse spatial distribution of gluons obtained from exclusive J/ψ production at the EIC.

1141 **Tomographic images of the proton:** By choosing particular final states in $e+p$ scattering, the EIC,
 1142 with its unprecedented luminosity and detector coverage, will create detailed images of the proton's gluon
 1143 matter distribution, as shown in the right panel of Figure 11. Such measurements would reveal aspects of
 1144 proton structure that are intimately connected with QCD dynamics at large distances.

1145 **QCD matter at extreme gluon density:** When fast moving hadrons are probed at high energy, the
 1146 low-momentum gluons contained in their wave functions become experimentally accessible. By colliding
 1147 electrons with heavy nuclei moving at light-speed, the EIC will provide access to a so far unconfirmed
 1148 regime of matter where abundant gluons dominate its behavior as shown in the left panel of Figure 12.
 1149 Such cold gluon matter is an emergent phenomenon of QCD dynamics and of high scientific interest and
 1150 curiosity. Furthermore, its underlying QCD dynamics and its predicted universal properties are critically
 1151 important for understanding the dynamical origin of the creation of the QGP from colliding two relativistic
 1152 heavy ions.

1153 By measuring diffractive cross-sections together with the total deep-inelastic scattering (DIS) cross-
 1154 sections in $e+p$ and $e+A$ collisions, shown in the right panel of Figure 12, the EIC would provide the first
 1155 unambiguous evidence for this novel state of saturated gluon matter in QCD. The planned EIC is capable
 1156 of exploring with precision the new field of collective dynamics of saturated gluons at high energies.

1157 **Hadronization and energy loss:** The mechanism by which colored partons pass through colored media,
 1158 both cold nuclei and hot QGP matter, and color-singlet hadrons finally emerge from the colored partons
 1159 is not understood. A nucleus in the EIC would provide an invaluable femtometer filter to explore and
 1160 expose how colored partons interact and hadronize in nuclear matter, as illustrated in the left panel of
 1161 Figure 13. By measuring π and D^0 meson production in both $e+p$ and $e+A$ collisions, the EIC would

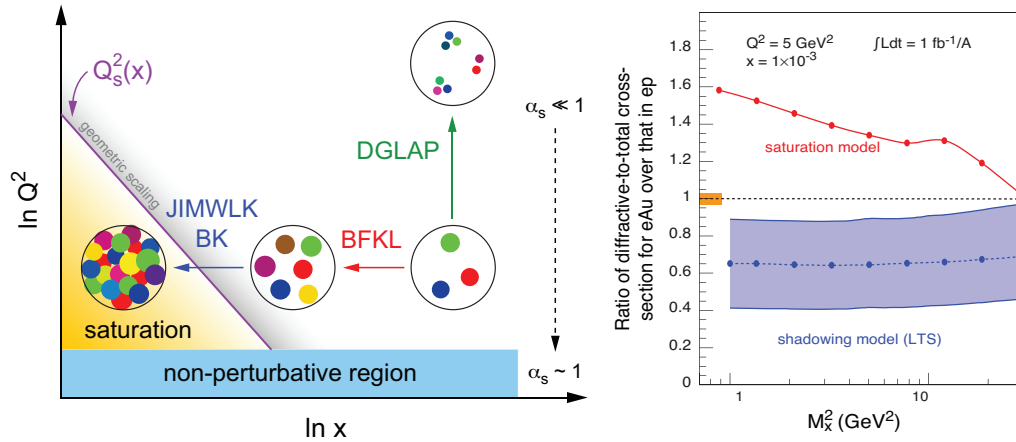


Figure 12: **Left panel:** Schematic landscape of probe resolution vs. energy, indicating regions of non-perturbative and perturbative QCD, including low to high parton density and the transition region. **Right panel:** Ratio of diffractive over total cross section for deep-inelastic scattering (DIS) of electrons on gold, normalized to DIS on the proton, for different values of the square of the invariant mass of the hadrons produced in the collisions, with and without saturation.

1162 provide the first measurement of the quark mass dependence of the response of nuclear matter to a fast
 1163 moving quark. The dramatic difference between them, shown in the right panel of Figure 13, would be
 1164 readily discernible. The color bands reflect the limitations on our current knowledge of hadronization –
 1165 the emergence of a pion from a colored quark. Enabling all such studies in one place, the EIC will be a
 1166 true QCD Laboratory, a unique facility in the world.

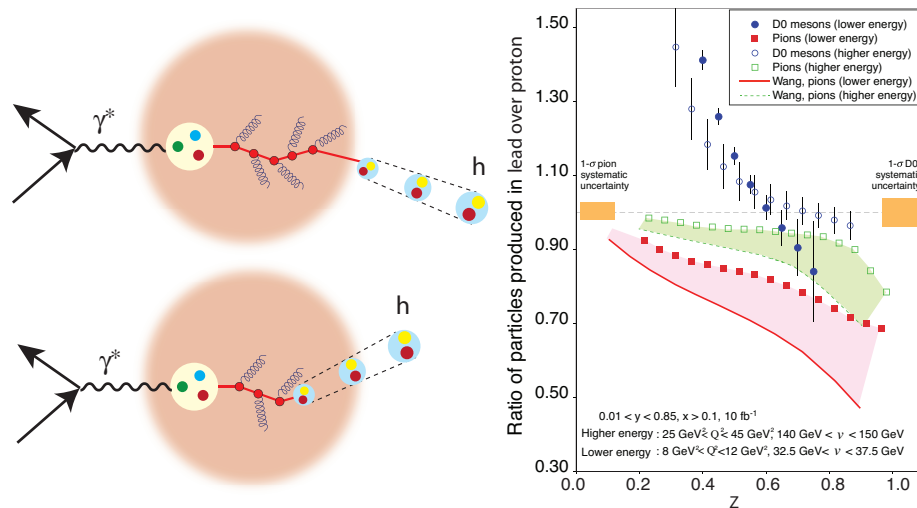


Figure 13: **Left panel:** A schematic illustrating the interaction of a parton moving through cold nuclear matter, where the hadron is formed outside (top) or inside the nucleus (bottom). **Right panel:** The ratio of the semi-inclusive cross sections for producing a pion (light quarks, red) and D^0 mesons (heavy quarks, blue) in e +lead collisions to e +deuteron collisions, plotted as a function of the ratio z of the momentum carried by the produced hadron to that of a virtual photon.

1167 4.3 EIC machine parameters and designs

1168 Two independent designs for a future EIC have evolved over the past few years. Both use existing
1169 infrastructure and facilities available to the US nuclear scientists. At Brookhaven National Laboratory
1170 (BNL), the eRHIC concept adds a new electron beam facility, based on an Energy Recovery Linac (ERL)
1171 to be built inside the RHIC tunnel, to collide electrons with one of the existing RHIC beams. At Jefferson
1172 Laboratory the Medium Energy Electron Ion Collider (MEIC) concept envisions a new electron and ion
1173 collider ring complex, together with the 12 GeV upgraded CEBAF, in order to achieve similar collision
1174 parameters. The machine designs aim to reach the following goals and parameters:

- 1175 • Polarized ($\sim 70\%$) beams of electrons, protons and light nuclei;
- 1176 • Ion beams from deuteron to the heaviest nuclei (uranium or lead);
- 1177 • Variable center of mass energies from ~ 20 to ~ 100 GeV, upgradable to ~ 140 GeV;
- 1178 • High collision luminosity $\sim 10^{33} - 10^{34} \text{ cm}^{-2}\text{sec}^{-1}$;
- 1179 • Capacity to have more than one interaction region.

1180 4.4 Why now?

1181 Today, a set of compelling physics questions related to role of gluons in QCD has been formulated,
1182 and a corresponding set of measurements at the EIC identified. A powerful formalism that connects
1183 those measurements to the QCD structure of hadrons and nuclei has been developed. The EIC was
1184 designated in the 2007 Nuclear Physics Long Range Plan as “*embodying the vision for reaching the next*
1185 *QCD frontier.*” In 2013 the NSAC Subcommittee report on Future Scientific Facilities declared an EIC
1186 to be “*absolutely essential in its ability to contribute to the world-leading science in the next decade.*”
1187 Accelerator technology has recently developed so that an EIC with the versatile range of kinematics,
1188 beam species and polarization, crucial to addressing the most central questions in QCD, can now be
1189 constructed at an affordable cost. Realizing the EIC will be essential to maintain U.S. leadership in the
1190 important fields of nuclear physics and accelerator science.

5 Bibliography

- 1191
- 1192 [1] A. Accardi, J. Albacete, M. Anselmino, N. Armesto, E. Aschenauer, et al., *Electron Ion Collider:*
1193 *The Next QCD Frontier - Understanding the glue that binds us all*, arXiv:1212.1701
1194 [nucl-ex].
- 1195 [2] A. P. Mishra, R. K. Mohapatra, P. Saumia, and A. M. Srivastava, *Super-horizon fluctuations and*
1196 *acoustic oscillations in relativistic heavy-ion collisions*, Phys. Rev. **C77** (2008) 064902,
1197 arXiv:0711.1323 [hep-ph].
- 1198 [3] S. A. Voloshin, *Transverse radial expansion in nuclear collisions and two particle correlations*, Phys.
1199 Lett. **B632** (2006) 490–494, arXiv:nucl-th/0312065 [nucl-th].
- 1200 [4] J. Takahashi, B. Tavares, W. Qian, R. Andrade, F. Grassi, et al., *Topology studies of*
1201 *hydrodynamics using two particle correlation analysis*, Phys. Rev. Lett. **103** (2009) 242301,
1202 arXiv:0902.4870 [nucl-th].
- 1203 [5] P. Sorensen, *Implications of space-momentum correlations and geometric fluctuations in heavy-ion*
1204 *collisions*, J. Phys. **G37** (2010) 094011, arXiv:1002.4878 [nucl-ex].
- 1205 [6] B. Alver and G. Roland, *Collision geometry fluctuations and triangular flow in heavy-ion collisions*,
1206 Phys. Rev. **C81** (2010) 054905, arXiv:1003.0194 [nucl-th].
- 1207 [7] ATLAS Collaboration, G. Aad et al., *Measurement of the azimuthal anisotropy for charged particle*
1208 *production in $\sqrt{s_{NN}} = 2.76$ TeV lead-lead collisions with the ATLAS detector*, Phys. Rev. **C86**
1209 (2012) 014907, arXiv:1203.3087 [hep-ex].
- 1210 [8] ALICE Collaboration, K. Aamodt et al., *Higher harmonic anisotropic flow measurements of*
1211 *charged particles in Pb-Pb collisions at $\sqrt{s_{NN}} = 2.76$ TeV*, Phys. Rev. Lett. **107** (2011) 032301,
1212 arXiv:1105.3865 [nucl-ex].
- 1213 [9] PHENIX Collaboration, A. Adare et al., *Measurements of Higher-Order Flow Harmonics in Au+Au*
1214 *Collisions at $\sqrt{s_{NN}} = 200$ GeV*, Phys. Rev. Lett. **107** (2011) 252301, arXiv:1105.3928
1215 [nucl-ex].
- 1216 [10] STAR Collaboration, L. Adamczyk et al., *Third Harmonic Flow of Charged Particles in Au+Au*
1217 *Collisions at $\sqrt{s_{NN}} = 200$ GeV*, Phys. Rev. **C88** (2013) no. 1, 014904, arXiv:1301.2187
1218 [nucl-ex].
- 1219 [11] STAR Collaboration, C. Adler et al., *Elliptic flow from two and four particle correlations in Au+Au*
1220 *collisions at $\sqrt{s_{NN}} = 130$ -GeV*, Phys. Rev. **C66** (2002) 034904,
1221 arXiv:nucl-ex/0206001 [nucl-ex].
- 1222 [12] M. Miller and R. Snellings, *Eccentricity fluctuations and its possible effect on elliptic flow*
1223 *measurements*, arXiv:nucl-ex/0312008 [nucl-ex].
- 1224 [13] B. Alver, B. Back, M. Baker, M. Ballintijn, D. Barton, et al., *Importance of correlations and*
1225 *fluctuations on the initial source eccentricity in high-energy nucleus-nucleus collisions*, Phys. Rev.
1226 **C77** (2008) 014906, arXiv:0711.3724 [nucl-ex].
- 1227 [14] U. Heinz and R. Snellings, *Collective flow and viscosity in relativistic heavy-ion collisions*, Annu.
1228 Rev. Nucl. Part. Sci. **63** (2013) 123–151, arXiv:1301.2826 [nucl-th].
- 1229 [15] D. Teaney, *The Effects of viscosity on spectra, elliptic flow, and HBT radii*, Phys. Rev. **C68** (2003)
1230 034913, arXiv:nucl-th/0301099 [nucl-th].
- 1231 [16] P. Romatschke and U. Romatschke, *Viscosity Information from Relativistic Nuclear Collisions: How*

- 1232 *Perfect is the Fluid Observed at RHIC?*, Phys. Rev. Lett. **99** (2007) 172301, arXiv:0706.1522
1233 [nucl-th].
- 1234 [17] H. Song, S. A. Bass, U. Heinz, T. Hirano, and C. Shen, *200 A GeV Au+Au collisions serve a nearly*
1235 *perfect quark-gluon liquid*, Phys. Rev. Lett. **106** (2011) 192301, arXiv:1011.2783 [nucl-th].
- 1236 [18] P. Kovtun, D. T. Son, and A. O. Starinets, *Viscosity in strongly interacting quantum field theories*
1237 *from black hole physics*, Phys. Rev. Lett. **94** (2005) 111601, arXiv:hep-th/0405231 [hep-th].
- 1238 [19] U. W. Heinz, *Towards the Little Bang Standard Model*, J. Phys. Conf. Ser. **455** (2013) 012044,
1239 arXiv:1304.3634 [nucl-th].
- 1240 [20] B. Schenke, S. Jeon, and C. Gale, *Elliptic and triangular flow in event-by-event (3+1)D viscous*
1241 *hydrodynamics*, Phys. Rev. Lett. **106** (2011) 042301, arXiv:1009.3244 [hep-ph].
- 1242 [21] H. Song, S. A. Bass, and U. Heinz, *Viscous QCD matter in a hybrid hydrodynamic+Boltzmann*
1243 *approach*, Phys. Rev. **C83** (2011) 024912, arXiv:1012.0555 [nucl-th].
- 1244 [22] B. Schenke, S. Jeon, and C. Gale, *Higher flow harmonics from (3+1)D event-by-event viscous*
1245 *hydrodynamics*, Phys. Rev. **C85** (2012) 024901, arXiv:1109.6289 [hep-ph].
- 1246 [23] B. Schenke, P. Tribedy, and R. Venugopalan, *Fluctuating Glasma initial conditions and flow in*
1247 *heavy ion collisions*, Phys. Rev. Lett. **108** (2012) 252301, arXiv:1202.6646 [nucl-th].
- 1248 [24] C. Gale, S. Jeon, B. Schenke, P. Tribedy, and R. Venugopalan, *Event-by-event anisotropic flow in*
1249 *heavy-ion collisions from combined Yang-Mills and viscous fluid dynamics*, Phys. Rev. Lett. **110**
1250 (2013) 012302, arXiv:1209.6330 [nucl-th].
- 1251 [25] H. Song, F. Meng, X. Xin, and Y.-X. Liu, *Elliptic flow of Λ , Ξ and Ω in 2.76 A TeV Pb+Pb*
1252 *collisions*, J. Phys. Conf. Ser. **509** (2014) 012089, arXiv:1310.3462 [nucl-th].
- 1253 [26] H. Song, S. Bass, and U. W. Heinz, *Spectra and elliptic flow for identified hadrons in 2.76A TeV*
1254 *Pb + Pb collisions*, Phys. Rev. **C89** (2014) no. 3, 034919, arXiv:1311.0157 [nucl-th].
- 1255 [27] W. van der Schee, P. Romatschke, and S. Pratt, *Fully Dynamical Simulation of Central Nuclear*
1256 *Collisions*, Phys. Rev. Lett. **111** (2013) no. 22, 222302, arXiv:1307.2539.
- 1257 [28] M. Habich, J. Nagle, and P. Romatschke, *Particle spectra and HBT radii for simulated central*
1258 *nuclear collisions of C+C, Al+Al, Cu+Cu, Au+Au, and Pb+Pb from Sqrt(s)=62.4-2760 GeV*,
1259 arXiv:1409.0040 [nucl-th].
- 1260 [29] A. Bazavov, T. Bhattacharya, M. Cheng, N. Christ, C. DeTar, et al., *Equation of state and QCD*
1261 *transition at finite temperature*, Phys. Rev. **D80** (2009) 014504, arXiv:0903.4379 [hep-lat].
- 1262 [30] S. Borsanyi, G. Endrodi, Z. Fodor, A. Jakovac, S. D. Katz, et al., *The QCD equation of state with*
1263 *dynamical quarks*, JHEP **1011** (2010) 077, arXiv:1007.2580 [hep-lat].
- 1264 [31] S. Borsanyi, Z. Fodor, C. Hoelbling, S. D. Katz, S. Krieg, et al., *Full result for the QCD equation*
1265 *of state with 2+1 flavors*, Phys.Lett. **B730** (2014) 99–104, arXiv:1309.5258 [hep-lat].
- 1266 [32] HotQCD Collaboration, A. Bazavov et al., *Equation of state in (2+1)-flavor QCD*, Phys. Rev.
1267 **D90** (2014) no. 9, 094503, arXiv:1407.6387 [hep-lat].
- 1268 [33] C. Gale, S. Jeon, and B. Schenke, *Hydrodynamic Modeling of Heavy-Ion Collisions*, Int. J. Mod.
1269 Phys. **A28** (2013) 1340011, arXiv:1301.5893 [nucl-th].
- 1270 [34] R. S. Bhalerao, M. Luzum, and J.-Y. Ollitrault, *Determining initial-state fluctuations from flow*
1271 *measurements in heavy-ion collisions*, Phys. Rev. **C84** (2011) 034910, arXiv:1104.4740
1272 [nucl-th].

- 1273 [35] J. Jia, *Event-shape fluctuations and flow correlations in ultra-relativistic heavy-ion collisions*,
1274 J. Phys. G **41** (2014) 124003, arXiv:1407.6057 [nucl-ex].
- 1275 [36] R. S. Bhalerao, J.-Y. Ollitrault, and S. Pal, *Characterizing flow fluctuations with moments*,
1276 arXiv:1411.5160 [nucl-th].
- 1277 [37] ATLAS, G. Aad et al., *Measurement of the distributions of event-by-event flow harmonics in*
1278 *lead-lead collisions at $\sqrt{s_{NN}} = 2.76$ TeV with the ATLAS detector at the LHC*, JHEP **1311** (2013) 183,
1279 arXiv:1305.2942 [hep-ex].
- 1280 [38] ATLAS Collaboration, G. Aad et al., *Measurement of event-plane correlations in $\sqrt{s_{NN}} = 2.76$*
1281 *TeV lead-lead collisions with the ATLAS detector*, Phys. Rev. **C90** (2014) no. 2, 024905,
1282 arXiv:1403.0489 [hep-ex].
- 1283 [39] CMS Collaboration, S. Chatrchyan et al., *Studies of azimuthal dihadron correlations in*
1284 *ultra-central PbPb collisions at $\sqrt{s_{NN}} = 2.76$ TeV*, arXiv:1312.1845 [nucl-ex].
- 1285 [40] U. Heinz, Z. Qiu, and C. Shen, *Fluctuating flow angles and anisotropic flow measurements*, Phys.
1286 Rev. **C87** (2013) no. 3, 034913, arXiv:1302.3535 [nucl-th].
- 1287 [41] Z. Qiu and U. Heinz, *Hydrodynamic event-plane correlations in Pb+Pb collisions at*
1288 *$\sqrt{s} = 2.76$ ATeV*, Phys. Lett. **B717** (2012) 261, arXiv:1208.1200 [nucl-th].
- 1289 [42] R. S. Bhalerao, J.-Y. Ollitrault, and S. Pal, *Event-plane correlators*, Phys. Rev. **C88** (2013)
1290 024909, arXiv:1307.0980 [nucl-th].
- 1291 [43] J. Novak, K. Novak, S. Pratt, J. Vredevoogd, C. Coleman-Smith, et al., *Determining Fundamental*
1292 *Properties of Matter Created in Ultrarelativistic Heavy-Ion Collisions*, Phys. Rev. **C89** (2014)
1293 034917, arXiv:1303.5769 [nucl-th].
- 1294 [44] C. Shen, U. W. Heinz, J.-F. Paquet, and C. Gale, *Thermal photons as a quark-gluon plasma*
1295 *thermometer reexamined*, Phys. Rev. **C89** (2014) no. 4, 044910, arXiv:1308.2440 [nucl-th].
- 1296 [45] C. Shen, U. Heinz, J.-F. Paquet, and C. Gale, *Thermal photon anisotropic flow serves as a*
1297 *quark-gluon plasma viscometer*, arXiv:1403.7558 [nucl-th].
- 1298 [46] PHENIX Collaboration, A. Adare et al., *Observation of direct-photon collective flow in*
1299 *$\sqrt{s_{NN}} = 200$ GeV Au+Au collisions*, Phys. Rev. Lett. **109** (2012) 122302, arXiv:1105.4126
1300 [nucl-ex].
- 1301 [47] ALICE Collaboration, D. Lohner, *Measurement of Direct-Photon Elliptic Flow in Pb-Pb Collisions*
1302 *at $\sqrt{s_{NN}} = 2.76$ TeV*, J. Phys. Conf. Ser. **446** (2013) 012028, arXiv:1212.3995 [hep-ex].
- 1303 [48] H. van Hees, M. He, and R. Rapp, *Pseudo-Critical Enhancement of Thermal Photons in*
1304 *Relativistic Heavy-Ion Collisions*, Nucl. Phys. **A933** (2014) 256, arXiv:1404.2846 [nucl-th].
- 1305 [49] CMS Collaboration, V. Khachatryan et al., *Observation of Long-Range Near-Side Angular*
1306 *Correlations in Proton-Proton Collisions at the LHC*, JHEP **1009** (2010) 091, arXiv:1009.4122
1307 [hep-ex].
- 1308 [50] CMS Collaboration, S. Chatrchyan et al., *Observation of long-range near-side angular correlations*
1309 *in proton-lead collisions at the LHC*, Phys. Lett. **B718** (2013) 795–814, arXiv:1210.5482
1310 [nucl-ex].
- 1311 [51] ALICE Collaboration, B. Abelev et al., *Long-range angular correlations on the near and away side*
1312 *in p-Pb collisions at $\sqrt{s_{NN}} = 5.02$ TeV*, Phys. Lett. **B719** (2013) 29–41, arXiv:1212.2001
1313 [nucl-ex].

- 1314 [52] ATLAS Collaboration, G. Aad et al., *Observation of Associated Near-Side and Away-Side*
1315 *Long-Range Correlations in $\sqrt{s_{NN}}=5.02\text{TeV}$ Proton-Lead Collisions with the ATLAS Detector,*
1316 *Phys. Rev. Lett.* **110** (2013) no. 18, 182302, arXiv:1212.5198 [hep-ex].
- 1317 [53] PHENIX Collaboration, A. Adare et al., *Quadrupole Anisotropy in Dihadron Azimuthal*
1318 *Correlations in Central $d+Au$ Collisions at $\sqrt{s_{NN}}=200$ GeV,* *Phys. Rev. Lett.* **111** (2013) no. 21,
1319 212301, arXiv:1303.1794 [nucl-ex].
- 1320 [54] ATLAS Collaboration, G. Aad et al., *Measurement with the ATLAS detector of multi-particle*
1321 *azimuthal correlations in $p+Pb$ collisions at $\sqrt{s_{NN}}=5.02$ TeV,* *Phys. Lett.* **B725** (2013) 60–78,
1322 arXiv:1303.2084 [hep-ex].
- 1323 [55] CMS Collaboration, S. Chatrchyan et al., *Multiplicity and transverse momentum dependence of*
1324 *two- and four-particle correlations in pPb and $PbPb$ collisions,* *Phys. Lett.* **B724** (2013) 213–240,
1325 arXiv:1305.0609 [nucl-ex].
- 1326 [56] ALICE Collaboration, B. B. Abelev et al., *Multiparticle azimuthal correlations in $p-Pb$ and $Pb-Pb$*
1327 *collisions at the CERN Large Hadron Collider,* *Phys. Rev.* **C90** (2014) no. 5, 054901,
1328 arXiv:1406.2474 [nucl-ex].
- 1329 [57] ATLAS Collaboration, G. Aad et al., *Measurement of long-range pseudorapidity correlations and*
1330 *azimuthal harmonics in $\sqrt{s_{NN}} = 5.02$ TeV proton-lead collisions with the ATLAS detector,* *Phys.*
1331 *Rev.* **C90** (2014) no. 4, 044906, arXiv:1409.1792 [hep-ex].
- 1332 [58] ALICE Collaboration, B. B. Abelev et al., *Long-range angular correlations of π , K and p in $p-Pb$*
1333 *collisions at $\sqrt{s_{NN}} = 5.02$ TeV,* *Phys. Lett.* **B726** (2013) 164–177, arXiv:1307.3237
1334 [nucl-ex].
- 1335 [59] CMS Collaboration, V. Khachatryan et al., *Long-range two-particle correlations of strange hadrons*
1336 *with charged particles in pPb and $PbPb$ collisions at LHC energies,* arXiv:1409.3392
1337 [nucl-ex].
- 1338 [60] CMS Collaboration, *Multiplicity dependence of multiparticle correlations in pPb and $PbPb$*
1339 *collisions,* .
- 1340 [61] H. Niemi and G. Denicol, *How large is the Knudsen number reached in fluid dynamical simulations*
1341 *of ultrarelativistic heavy ion collisions?,* arXiv:1404.7327 [nucl-th].
- 1342 [62] Y. Aoki, G. Endrodi, Z. Fodor, S. Katz, and K. Szabo, *The Order of the quantum*
1343 *chromodynamics transition predicted by the standard model of particle physics,* *Nature* **443** (2006)
1344 675–678, arXiv:hep-lat/0611014 [hep-lat].
- 1345 [63] Y. Aoki, S. Borsanyi, S. Durr, Z. Fodor, S. D. Katz, et al., *The QCD transition temperature:*
1346 *results with physical masses in the continuum limit II.,* *JHEP* **0906** (2009) 088,
1347 arXiv:0903.4155 [hep-lat].
- 1348 [64] A. Bazavov, T. Bhattacharya, M. Cheng, C. DeTar, H. Ding, et al., *The chiral and deconfinement*
1349 *aspects of the QCD transition,* *Phys.Rev.* **D85** (2012) 054503, arXiv:1111.1710 [hep-lat].
- 1350 [65] M. A. Stephanov, K. Rajagopal, and E. V. Shuryak, *Signatures of the tricritical point in QCD,*
1351 *Phys. Rev. Lett.* **81** (1998) 4816–4819, arXiv:hep-ph/9806219 [hep-ph].
- 1352 [66] Z. Fodor and S. Katz, *Critical point of QCD at finite T and μ , lattice results for physical quark*
1353 *masses,* *JHEP* **0404** (2004) 050, arXiv:hep-lat/0402006 [hep-lat].
- 1354 [67] C. Allton, M. Doring, S. Ejiri, S. Hands, O. Kaczmarek, et al., *Thermodynamics of two flavor QCD*
1355 *to sixth order in quark chemical potential,* *Phys. Rev.* **D71** (2005) 054508,

- 1356 arXiv:hep-lat/0501030 [hep-lat].
- 1357 [68] R. Gavai and S. Gupta, *QCD at finite chemical potential with six time slices*, Phys. Rev. **D78**
1358 (2008) 114503, arXiv:0806.2233 [hep-lat].
- 1359 [69] P. de Forcrand and O. Philipsen, *The curvature of the critical surface $(m(u,d),m(s))^{**crit}(\mu)$: A*
1360 *Progress report*, PoS **LATTICE2008** (2008) 208, arXiv:0811.3858 [hep-lat].
- 1361 [70] S. Datta, R. V. Gavai, and S. Gupta, *The QCD Critical Point : marching towards continuum*, Nucl.
1362 Phys. **A904-905** (2013) 883c–886c, arXiv:1210.6784 [hep-lat].
- 1363 [71] *Studying the Phase Diagram of QCD Matter at RHIC*, 2014.
1364 https://drupal.star.bnl.gov/STAR/files/BES_WPII_ver6.9_Cover.pdf.
- 1365 [72] STAR Collaboration, L. Kumar, *STAR Results from the RHIC Beam Energy Scan-I*, Nucl. Phys. A
1366 **904-905** (2013) 256c–263c, arXiv:1211.1350 [nucl-ex].
- 1367 [73] STAR Collaboration, L. Adamczyk et al., *Beam energy dependent two-pion interferometry and the*
1368 *freeze-out eccentricity of pions in heavy ion collisions at STAR*, arXiv:1403.4972 [nucl-ex].
- 1369 [74] PHENIX Collaboration, A. Adare et al., *Beam-energy and system-size dependence of the*
1370 *space-time extent of the pion emission source produced in heavy ion collisions*, arXiv:1410.2559
1371 [nucl-ex].
- 1372 [75] ALICE Collaboration, K. Aamodt et al., *Two-pion Bose-Einstein correlations in central Pb-Pb*
1373 *collisions at $\sqrt{s_{NN}} = 2.76$ TeV*, Phys. Lett. **B696** (2011) 328–337, arXiv:1012.4035
1374 [nucl-ex].
- 1375 [76] D. H. Rischke and M. Gyulassy, *The Time delay signature of quark - gluon plasma formation in*
1376 *relativistic nuclear collisions*, Nucl. Phys. **A608** (1996) 479–512, arXiv:nucl-th/9606039
1377 [nucl-th].
- 1378 [77] STAR Collaboration, L. Adamczyk et al., *Energy Dependence of Moments of Net-proton*
1379 *Multiplicity Distributions at RHIC*, Phys. Rev. Lett. **112** (2014) no. 3, 032302, arXiv:1309.5681
1380 [nucl-ex].
- 1381 [78] STAR Collaboration, X. Luo, *Search for the QCD Critical Point: Energy Dependence of Higher*
1382 *Moments of Net-proton and Net-charge Distributions at RHIC*, .
1383 http://www.physik.uni-bielefeld.de/~cpod2014/CP0D2014_LuoXiaofeng_ver5.pdf.
1384 Talk at 2014 CPOD Conference.
- 1385 [79] M. Stephanov, *On the sign of kurtosis near the QCD critical point*, Phys. Rev. Lett. **107** (2011)
1386 052301, arXiv:1104.1627 [hep-ph].
- 1387 [80] STAR Collaboration, L. Adamczyk et al., *Beam-Energy Dependence of the Directed Flow of*
1388 *Protons, Antiprotons, and Pions in Au+Au Collisions*, Phys. Rev. Lett. **112** (2014) no. 16, 162301,
1389 arXiv:1401.3043 [nucl-ex].
- 1390 [81] J. Brachmann, A. Dumitru, H. Stoecker, and W. Greiner, *The Directed flow maximum near $c(s) =$*
1391 *0*, Eur. Phys. J. **A8** (2000) 549–552, arXiv:nucl-th/9912014 [nucl-th].
- 1392 [82] H. Stoecker, *Collective flow signals the quark gluon plasma*, Nucl. Phys. **A750** (2005) 121–147,
1393 arXiv:nucl-th/0406018 [nucl-th].
- 1394 [83] P. Huovinen, P. Petreczky, and C. Schmidt, *Equation of state at finite net-baryon density using*
1395 *Taylor coefficients up to sixth order*, Nucl. Phys. **A931** (2014) no. 0, 769 – 773.
1396 <http://www.sciencedirect.com/science/article/pii/S0375947414003297>. {QUARK}
1397 {MATTER} 2014 {XXIV} {INTERNATIONAL} {CONFERENCE} {ON}

- 1398 {ULTRARELATIVISTIC} NUCLEUS-NUCLEUS {COLLISIONS}.
- 1399 [84] STAR Collaboration, B. Abelev et al., *Partonic flow and phi-meson production in Au + Au*
1400 *collisions at $s(NN)^{1/2} = 200$ -GeV*, Phys. Rev. Lett. **99** (2007) 112301,
1401 arXiv:nucl-ex/0703033 [NUCL-EX].
- 1402 [85] STAR Collaboration, B. Abelev et al., *Azimuthal Charged-Particle Correlations and Possible Local*
1403 *Strong Parity Violation*, Phys. Rev. Lett. **103** (2009) 251601, arXiv:0909.1739 [nucl-ex].
- 1404 [86] ALICE Collaboration, B. Abelev et al., *Charge separation relative to the reaction plane in Pb-Pb*
1405 *collisions at $\sqrt{s_{NN}} = 2.76$ TeV*, Phys. Rev. Lett. **110** (2013) 012301, arXiv:1207.0900
1406 [nucl-ex].
- 1407 [87] STAR Collaboration, L. Adamczyk et al., *Measurement of Charge Multiplicity Asymmetry*
1408 *Correlations in High Energy Nucleus-Nucleus Collisions at 200 GeV*, Phys. Rev. **C89** (2014)
1409 044908, arXiv:1303.0901 [nucl-ex].
- 1410 [88] K. Fukushima, D. E. Kharzeev, and H. J. Warringa, *The Chiral Magnetic Effect*, Phys. Rev. **D78**
1411 (2008) 074033, arXiv:0808.3382 [hep-ph].
- 1412 [89] D. E. Kharzeev and D. T. Son, *Testing the chiral magnetic and chiral vortical effects in heavy ion*
1413 *collisions*, Phys. Rev. Lett. **106** (2011) 062301, arXiv:1010.0038 [hep-ph].
- 1414 [90] A. Bzdak, V. Koch, and J. Liao, *Remarks on possible local parity violation in heavy ion collisions*,
1415 Phys. Rev. **C81** (2010) 031901, arXiv:0912.5050 [nucl-th].
- 1416 [91] S. Pratt, S. Schlichting, and S. Gavin, *Effects of Momentum Conservation and Flow on Angular*
1417 *Correlations at RHIC*, Phys. Rev. **C84** (2011) 024909, arXiv:1011.6053 [nucl-th].
- 1418 [92] STAR Collaboration, L. Adamczyk et al., *Beam-energy dependence of charge separation along the*
1419 *magnetic field in Au+Au collisions at RHIC*, Phys. Rev. Lett. **113** (2014) 052302,
1420 arXiv:1404.1433 [nucl-ex].
- 1421 [93] M. D'Elia, S. Mukherjee, and F. Sanfilippo, *QCD Phase Transition in a Strong Magnetic*
1422 *Background*, Phys. Rev. **D82** (2010) 051501, arXiv:1005.5365 [hep-lat].
- 1423 [94] G. Bali, F. Bruckmann, G. Endrodi, Z. Fodor, S. Katz, et al., *The QCD phase diagram for external*
1424 *magnetic fields*, JHEP **1202** (2012) 044, arXiv:1111.4956 [hep-lat].
- 1425 [95] G. Bali, F. Bruckmann, G. Endrödi, S. Katz, and A. Schäfer, *The QCD equation of state in*
1426 *background magnetic fields*, JHEP **1408** (2014) 177, arXiv:1406.0269 [hep-lat].
- 1427 [96] D. E. Kharzeev and H.-U. Yee, *Chiral Magnetic Wave*, Phys. Rev. **D83** (2011) 085007,
1428 arXiv:1012.6026 [hep-th].
- 1429 [97] Y. Burnier, D. E. Kharzeev, J. Liao, and H.-U. Yee, *Chiral magnetic wave at finite baryon density*
1430 *and the electric quadrupole moment of quark-gluon plasma in heavy ion collisions*, Phys. Rev. Lett.
1431 **107** (2011) 052303, arXiv:1103.1307 [hep-ph].
- 1432 [98] STAR Collaboration, G. Wang, *Search for Chiral Magnetic Effects in High-Energy Nuclear*
1433 *Collisions*, Nucl.Phys. **A904-905** (2013) 248c–255c, arXiv:1210.5498 [nucl-ex].
- 1434 [99] ALICE Collaboration, R. Belmont, *Charge-dependent anisotropic flow studies and the search for*
1435 *the Chiral Magnetic Wave in ALICE*, arXiv:1408.1043 [nucl-ex].
- 1436 [100] M. Stephanov, *Non-Gaussian fluctuations near the QCD critical point*, Phys. Rev. Lett. **102**
1437 (2009) 032301, arXiv:0809.3450 [hep-ph].
- 1438 [101] C. Athanasiou, K. Rajagopal, and M. Stephanov, *Using Higher Moments of Fluctuations and their*

- 1439 *Ratios in the Search for the QCD Critical Point*, Phys. Rev. **D82** (2010) 074008,
1440 arXiv:1006.4636 [hep-ph].
- 1441 [102] S. Ejiri, F. Karsch, and K. Redlich, *Hadronic fluctuations at the QCD phase transition*, Phys. Lett.
1442 **B633** (2006) 275–282, arXiv:hep-ph/0509051 [hep-ph].
- 1443 [103] F. Karsch and K. Redlich, *Probing freeze-out conditions in heavy ion collisions with moments of*
1444 *charge fluctuations*, Phys. Lett. **B695** (2011) 136–142, arXiv:1007.2581 [hep-ph].
- 1445 [104] STAR Collaboration, L. Adamczyk et al., *Beam energy dependence of moments of the net-charge*
1446 *multiplicity distributions in Au+Au collisions at RHIC*, Phys. Rev. Lett. **113** (2014) 092301,
1447 arXiv:1402.1558 [nucl-ex].
- 1448 [105] B. Berdnikov and K. Rajagopal, *Slowing out-of-equilibrium near the QCD critical point*, Phys. Rev.
1449 **D61** (2000) 105017, arXiv:hep-ph/9912274 [hep-ph].
- 1450 [106] F. Karsch, *Determination of Freeze-out Conditions from Lattice QCD Calculations*, Central Eur. J.
1451 Phys. **10** (2012) 1234–1237, arXiv:1202.4173 [hep-lat].
- 1452 [107] A. Bazavov, H. Ding, P. Hegde, O. Kaczmarek, F. Karsch, et al., *Freeze-out Conditions in Heavy*
1453 *Ion Collisions from QCD Thermodynamics*, Phys. Rev. Lett. **109** (2012) 192302,
1454 arXiv:1208.1220 [hep-lat].
- 1455 [108] S. Mukherjee and M. Wagner, *Deconfinement of strangeness and freeze-out from charge*
1456 *fluctuations*, PoS **CPOD2013** (2013) 039, arXiv:1307.6255 [nucl-th].
- 1457 [109] S. Borsanyi, Z. Fodor, S. Katz, S. Krieg, C. Ratti, et al., *Freeze-out parameters: lattice meets*
1458 *experiment*, Phys. Rev. Lett. **111** (2013) 062005, arXiv:1305.5161 [hep-lat].
- 1459 [110] S. Borsanyi, Z. Fodor, S. Katz, S. Krieg, C. Ratti, et al., *Freeze-out parameters from electric*
1460 *charge and baryon number fluctuations: is there consistency?*, Phys. Rev. Lett. **113** (2014)
1461 052301, arXiv:1403.4576 [hep-lat].
- 1462 [111] P. Huck, *Beam energy dependence of dielectron production in Au+Au collisions from {STAR} at*
1463 *{RHIC}*, Nuclear Physics A **931** (2014) 659 – 664, arXiv:1409.5675 [nucl-ex].
- 1464 [112] R. Rapp, J. Wambach, and H. van Hees, *The Chiral Restoration Transition of QCD and Low Mass*
1465 *Dileptons*, arXiv:0901.3289 [hep-ph].
- 1466 [113] S. Borsanyi, Z. Fodor, S. D. Katz, S. Krieg, C. Ratti, et al., *Fluctuations of conserved charges at*
1467 *finite temperature from lattice QCD*, JHEP **1201** (2012) 138, arXiv:1112.4416 [hep-lat].
- 1468 [114] HotQCD Collaboration, A. Bazavov et al., *Fluctuations and Correlations of net baryon number,*
1469 *electric charge, and strangeness: A comparison of lattice QCD results with the hadron resonance*
1470 *gas model*, Phys. Rev. **D86** (2012) 034509, arXiv:1203.0784 [hep-lat].
- 1471 [115] S. Borsanyi, G. Endrodi, Z. Fodor, S. Katz, S. Krieg, et al., *QCD equation of state at nonzero*
1472 *chemical potential: continuum results with physical quark masses at order mu^2* , JHEP **1208**
1473 (2012) 053, arXiv:1204.6710 [hep-lat].
- 1474 [116] for the BNL-Bielefeld-CCNU collaboration, P. Hegde, *The QCD equation of state to $\mathcal{O}(\mu_B^4)$* ,
1475 arXiv:1412.6727 [hep-lat].
- 1476 [117] G. F. Sterman and S. Weinberg, *Jets from Quantum Chromodynamics*, Phys. Rev. Lett. **39** (1977)
1477 1436.
- 1478 [118] R. Feynman, R. Field, and G. Fox, *A Quantum Chromodynamic Approach for the Large Transverse*
1479 *Momentum Production of Particles and Jets*, Phys. Rev. **D18** (1978) 3320.

- 1480 [119] R. Field and R. Feynman, *A Parametrization of the Properties of Quark Jets*, Nucl. Phys. **B136**
1481 (1978) 1.
- 1482 [120] PHENIX Collaboration, K. Adcox et al., *Suppression of hadrons with large transverse momentum*
1483 *in central Au+Au collisions at $\sqrt{s_{NN}} = 130$ -GeV*, Phys. Rev. Lett. **88** (2002) 022301,
1484 arXiv:nucl-ex/0109003 [nucl-ex].
- 1485 [121] STAR Collaboration, C. Adler et al., *Disappearance of back-to-back high p_T hadron correlations in*
1486 *central Au+Au collisions at $\sqrt{s_{NN}} = 200$ -GeV*, Phys. Rev. Lett. **90** (2003) 082302,
1487 arXiv:nucl-ex/0210033 [nucl-ex].
- 1488 [122] J. Bjorken, *Energy Loss of Energetic Partons in Quark - Gluon Plasma: Possible Extinction of High*
1489 *$p(t)$ Jets in Hadron - Hadron Collisions*, .
- 1490 [123] M. Gyulassy and X.-n. Wang, *Multiple collisions and induced gluon Bremsstrahlung in QCD*, Nucl.
1491 Phys. **B420** (1994) 583–614, arXiv:nucl-th/9306003 [nucl-th].
- 1492 [124] X.-N. Wang and M. Gyulassy, *Gluon shadowing and jet quenching in $A + A$ collisions at $s^{**}(1/2)$*
1493 *$= 200$ -GeV*, Phys. Rev. Lett. **68** (1992) 1480–1483.
- 1494 [125] R. Baier, Y. L. Dokshitzer, A. H. Mueller, S. Peigne, and D. Schiff, *Radiative energy loss of*
1495 *high-energy quarks and gluons in a finite volume quark - gluon plasma*, Nucl. Phys. **B483** (1997)
1496 291–320, arXiv:hep-ph/9607355 [hep-ph].
- 1497 [126] R. Baier, Y. L. Dokshitzer, A. H. Mueller, S. Peigne, and D. Schiff, *Radiative energy loss and $p(T)$*
1498 *broadening of high-energy partons in nuclei*, Nucl. Phys. **B484** (1997) 265–282,
1499 arXiv:hep-ph/9608322 [hep-ph].
- 1500 [127] B. Zakharov, *Fully quantum treatment of the Landau-Pomeranchuk-Migdal effect in QED and*
1501 *QCD*, JETP Lett. **63** (1996) 952–957, arXiv:hep-ph/9607440 [hep-ph].
- 1502 [128] B. Zakharov, *Radiative energy loss of high-energy quarks in finite size nuclear matter and quark -*
1503 *gluon plasma*, JETP Lett. **65** (1997) 615–620, arXiv:hep-ph/9704255 [hep-ph].
- 1504 [129] P. M. Chesler, K. Jensen, A. Karch, and L. G. Yaffe, *Light quark energy loss in strongly-coupled N*
1505 *$= 4$ supersymmetric Yang-Mills plasma*, Phys. Rev. **D79** (2009) 125015, arXiv:0810.1985
1506 [hep-th].
- 1507 [130] P. M. Chesler, K. Jensen, and A. Karch, *Jets in strongly-coupled $N = 4$ super Yang-Mills theory*,
1508 Phys. Rev. **D79** (2009) 025021, arXiv:0804.3110 [hep-th].
- 1509 [131] J. J. Friess, S. S. Gubser, and G. Michalogiorgakis, *Dissipation from a heavy quark moving through*
1510 *$N=4$ super-Yang-Mills plasma*, JHEP **0609** (2006) 072, arXiv:hep-th/0605292 [hep-th].
- 1511 [132] J. Casalderrey-Solana and D. Teaney, *Heavy quark diffusion in strongly coupled $N=4$ Yang-Mills*,
1512 Phys. Rev. **D74** (2006) 085012, arXiv:hep-ph/0605199 [hep-ph].
- 1513 [133] R. Baier, *Jet quenching*, Nucl. Phys. **A715** (2003) 209–218, arXiv:hep-ph/0209038 [hep-ph].
- 1514 [134] A. Majumder, *Elastic energy loss and longitudinal straggling of a hard jet*, Phys. Rev. **C80** (2009)
1515 031902, arXiv:0810.4967 [nucl-th].
- 1516 [135] JET Collaboration, K. M. Burke et al., *Extracting the jet transport coefficient from jet quenching*
1517 *in high-energy heavy-ion collisions*, Phys. Rev. **C90** (2014) no. 1, 014909, arXiv:1312.5003
1518 [nucl-th].
- 1519 [136] S. A. Bass, C. Gale, A. Majumder, C. Nonaka, G.-Y. Qin, et al., *Systematic Comparison of Jet*
1520 *Energy-Loss Schemes in a realistic hydrodynamic medium*, Phys. Rev. **C79** (2009) 024901,

- 1521 arXiv:0808.0908 [nucl-th].
- 1522 [137] sPHENIX Science Proposal, 2014. [http://www.phenix.bnl.gov/phenix/WWW/publish/](http://www.phenix.bnl.gov/phenix/WWW/publish/documents/sPHENIX_proposal_19112014.pdf)
1523 documents/sPHENIX_proposal_19112014.pdf.
- 1524 [138] ATLAS Collaboration, G. Aad et al., *Observation of a Centrality-Dependent Dijet Asymmetry in*
1525 *Lead-Lead Collisions at $\sqrt{s_{NN}} = 2.77$ TeV with the ATLAS Detector at the LHC*, Phys. Rev. Lett.
1526 **105** (2010) 252303, arXiv:1011.6182 [hep-ex].
- 1527 [139] CMS Collaboration, S. Chatrchyan et al., *Observation and studies of jet quenching in PbPb*
1528 *collisions at nucleon-nucleon center-of-mass energy = 2.76 TeV*, Phys. Rev. C **84** (2011) 024906,
1529 arXiv:1102.1957 [nucl-ex].
- 1530 [140] CMS Collaboration, S. Chatrchyan et al., *Studies of jet quenching using isolated-photon+jet*
1531 *correlations in PbPb and pp collisions at $\sqrt{s_{NN}} = 2.76$ TeV*, Phys. Lett. B **718** (2013) 773,
1532 arXiv:1205.0206 [nucl-ex].
- 1533 [141] ATLAS Collaboration, P. Steinberg, *Centrality, rapidity and pT dependence of isolated prompt*
1534 *photon production in lead-lead collisions at $s_{NN}=2.76$ TeV with the ATLAS detector at the LHC*,
1535 Nucl. Phys. **A931** (2014) 422–427.
- 1536 [142] PHENIX Collaboration, A. Adare et al., *Medium modification of jet fragmentation in Au + Au*
1537 *collisions at $\sqrt{s_{NN}} = 200$ GeV measured in direct photon-hadron correlations*, Phys. Rev. Lett.
1538 **111** (2013) no. 3, 032301, arXiv:1212.3323 [nucl-ex].
- 1539 [143] ATLAS Collaboration, G. Aad et al., *Measurement of the jet radius and transverse momentum*
1540 *dependence of inclusive jet suppression in lead-lead collisions at $\sqrt{s_{NN}} = 2.76$ TeV with the*
1541 *ATLAS detector*, Phys. Lett. **B719** (2013) 220–241, arXiv:1208.1967 [hep-ex].
- 1542 [144] CMS Collaboration, S. Chatrchyan et al., *Measurement of jet fragmentation into charged particles*
1543 *in pp and PbPb collisions at $\sqrt{s_{NN}} = 2.76$ TeV*, JHEP **1210** (2012) 087, arXiv:1205.5872
1544 [nucl-ex].
- 1545 [145] ALICE Collaboration, B. Abelev et al., *Suppression of high transverse momentum D mesons in*
1546 *central Pb-Pb collisions at $\sqrt{s_{NN}} = 2.76$ TeV*, JHEP **1209** (2012) 112, arXiv:1203.2160
1547 [nucl-ex].
- 1548 [146] CMS Collaboration, S. Chatrchyan et al., *Suppression of non-prompt J/ψ , prompt J/ψ , and $Y(1S)$*
1549 *in PbPb collisions at $\sqrt{s_{NN}} = 2.76$ TeV*, JHEP **1205** (2012) 063, arXiv:1201.5069
1550 [nucl-ex].
- 1551 [147] N. Brambilla, S. Eidelman, B. K. Heltsley, R. Vogt, G. T. Bodwin, et al., *Heavy quarkonium:*
1552 *progress, puzzles, and opportunities*, arXiv:arXiv:1010.5827 [hep-ph].
- 1553 [148] F. Karsch, M. Mehr, and H. Satz, *Color Screening and Deconfinement for Bound States of Heavy*
1554 *Quarks*, Z. Phys. **C37** (1988) 617.
- 1555 [149] A. Emerick, X. Zhao, and R. Rapp, *Bottomonia in the quark-gluon plasma and their production at*
1556 *RHIC and LHC*, arXiv:1111.6537 [hep-ph].
- 1557 [150] CMS Collaboration, S. Chatrchyan et al., *Indications of suppression of excited Υ states in PbPb*
1558 *collisions at $\sqrt{s_{NN}} = 2.76$ TeV*, Phys.Rev.Lett. **107** (2011) 052302, arXiv:1105.4894
1559 [nucl-ex].
- 1560 [151] PHENIX Collaboration, A. Adare et al., *Measurement of $\Upsilon(1S+2S+3S)$ production in p+p and*
1561 *Au+Au collisions at $\sqrt{s_{NN}} = 200$ GeV*, arXiv:1404.2246 [nucl-ex].
- 1562 [152] STAR Collaboration, L. Adamczyk et al., *Suppression of Upsilon Production in d+Au and Au+Au*

- 1563 *Collisions at $\sqrt{s_{NN}} = 200$ GeV*, Phys. Lett. **B735** (2014) 127, arXiv:1312.3675 [nucl-ex].
- 1564 [153] F. Gelis, E. Iancu, J. Jalilian-Marian, and R. Venugopalan, *The Color Glass Condensate*, Annu.
1565 Rev. Nucl. Part. Sci. **60** (2010) 463–489, arXiv:1002.0333 [hep-ph].
- 1566 [154] K. Dusling and R. Venugopalan, *Comparison of the color glass condensate to dihadron correlations*
1567 *in proton-proton and proton-nucleus collisions*, Phys. Rev. **D87** (2013) no. 9, 094034,
1568 arXiv:1302.7018 [hep-ph].
- 1569 [155] STAR Collaboration, *A Polarized p+p and p+A Program for the Next Years*, 2014.
1570 https://drupal.star.bnl.gov/STAR/files/pp.pA_.LoI_.pp_.pA_.v7.pdf.
- 1571 [156] PHENIX Collaboration, *Future Opportunities in p+p and p+A Collisions at RHIC with the Forward*
1572 *sPHENIX Detector*, . [http:](http://www.phenix.bnl.gov/phenix/WWW/publish/dave/sPHENIX/pp_pA_whitepaper.pdf)
1573 [//www.phenix.bnl.gov/phenix/WWW/publish/dave/sPHENIX/pp_pA_whitepaper.pdf](http://www.phenix.bnl.gov/phenix/WWW/publish/dave/sPHENIX/pp_pA_whitepaper.pdf).
- 1574 [157] F. Dominguez, C. Marquet, B.-W. Xiao, and F. Yuan, *Universality of Unintegrated Gluon*
1575 *Distributions at small x*, Phys. Rev. **D83** (2011) 105005, arXiv:1101.0715 [hep-ph].
- 1576 [158] Z.-B. Kang and F. Yuan, *Single Spin Asymmetry Scaling in the Forward Rapidity Region at RHIC*,
1577 Phys. Rev. **D84** (2011) 034019, arXiv:1106.1375 [hep-ph].
- 1578 [159] Y. V. Kovchegov and M. D. Sievert, *Sivers Function in the Quasi-Classical Approximation*, Phys.
1579 Rev. **D89** (2014) 054035, arXiv:1310.5028 [hep-ph].
- 1580 [160] E.-C. Aschenauer, S. Fazio, K. Kumericki, and D. Mueller, *Deeply Virtual Compton Scattering at a*
1581 *Proposed High-Luminosity Electron-Ion Collider*, JHEP **1309** (2013) 093, arXiv:1304.0077
1582 [hep-ph].
- 1583 [161] B. Schenke, P. Tribedy, and R. Venugopalan, *Event-by-event gluon multiplicity, energy density, and*
1584 *eccentricities in ultrarelativistic heavy-ion collisions*, Phys. Rev. **C86** (2012) 034908,
1585 arXiv:1206.6805 [hep-ph].
- 1586 [162] R. Paatelainen, K. Eskola, H. Niemi, and K. Tuominen, *Fluid dynamics with saturated minijet*
1587 *initial conditions in ultrarelativistic heavy-ion collisions*, Phys. Lett. **B731** (2014) 126–130,
1588 arXiv:1310.3105 [hep-ph].
- 1589 [163] Y. Aoki, Z. Fodor, S. Katz, and K. Szabo, *The QCD transition temperature: Results with physical*
1590 *masses in the continuum limit*, Phys. Lett. **B643** (2006) 46–54, arXiv:hep-lat/0609068
1591 [hep-lat].
- 1592 [164] G. Aarts, E. Seiler, and I.-O. Stamatescu, *The Complex Langevin method: When can it be*
1593 *trusted?*, Phys. Rev. **D81** (2010) 054508, arXiv:0912.3360 [hep-lat].
- 1594 [165] G. Aarts, F. Attanasio, B. Jäger, E. Seiler, D. Sexty, et al., *Exploring the phase diagram of QCD*
1595 *with complex Langevin simulations*, PoS **LATTICE2014** (2014) 200, arXiv:1411.2632
1596 [hep-lat].
- 1597 [166] AuroraScience Collaboration, M. Cristoforetti, F. Di Renzo, and L. Scorzato, *New approach to the*
1598 *sign problem in quantum field theories: High density QCD on a Lefschetz thimble*, Phys. Rev. **D86**
1599 (2012) 074506, arXiv:1205.3996 [hep-lat].
- 1600 [167] G. Aarts, L. Bongiovanni, E. Seiler, and D. Sexty, *Some remarks on Lefschetz thimbles and*
1601 *complex Langevin dynamics*, JHEP **1410** (2014) 159, arXiv:1407.2090 [hep-lat].

1602
1603

6 Appendix: Agenda of the “Phases of QCD Matter” and joint sessions at the QCD Town Meeting

Temple University QCD Town Meeting – Saturday, September 13, 2014			
“Phases of QCD Matter” meets separately	8:00 AM	Coffee, Tea, Bagels, Doughnuts and Fruit are Available	
	9:00 AM	Welcome and brief introduction to the format and goal of the meeting	Ulrich Heinz
	Theory Overview		
	9:10 AM	-- Open questions in theory, why they are interesting, what tools we have to address them	Krishna Rajagopal
			Discussion (10 min)
	9:50 AM	-- Lattice QCD for RHIC and LHC: from now to the next decade	Swagato Mukherjee
			Discussion (10min)
	10:30 AM	Coffee Break	
	QGP evolution and progress on EOS and transport properties		
	11:00 AM	-- The standard model for QGP evolution: theoretical status and future	Bjoern Schenke
			Discussion (10 min)
	11:40 AM	-- The standard model for QGP evolution: experimental status and future	Raimond Snellings
			Discussion (10 min)
	12:20 PM	Lunch Break	
	BES and QCD Phase Diagram		
	1:20 PM	-- BES I Results, Motivation for BES II, Future Facilities	Dan Cebra
			Discussion (10 min)
	2:00 AM	-- Studying the QCD Phase Diagram via BES	Misha Stephanov
	2:20 AM	-- Dynamical modeling at low collision energy and high μ_b	Hannah Petersen
			Discussion (10 min)
2:50 PM	Community Input (hot QCD related)		
3:30 PM	Coffee Break		
4:00 - 7:30 PM Joint Session			

Figure 14: Agenda of the “Phases of QCD Matter” parallel session, part I (Saturday)

Saturday		
Joint Hadronic and Phases of QCD Session		
4:00 PM	-- Nuclear theory for the next decade: an overview	David Kaplan
		Discussion (10 min)
4:40 PM	-- Highlights in cold QCD since 2007	Rolf Ent
5:00 PM	-- Cold QCD: the next decade	Naomi Makins
		Discussion (10 min)
5:30 PM	-- RHIC and LHC overview ("Where we are, where do we need to go?")	Bill Zajc
		Discussion (10 min)
6:20 PM	-- Why we need an EIC: a view from 30,000 feet	Berndt Mueller
6:40 PM	-- Why we need an EIC: a view from 10,000 meters	Bob McKeown
7:00 PM	Combined discussion period for the preceding 2 talks	Discussion (30 min)
Sunday		
Morning EIC Session		
8:30 AM	Central issues in nucleon structure (theory)	Xiangdong Ji
9:00 AM	Probing nucleon structure at an EIC	Zein-Eddine Meziani
9:30 AM	Probing the properties of QCD with atomic nuclei: theoretical perspective	Yuri Kovchegov
10:00 AM	Probing the properties of QCD with atomic nuclei: experimental perspective	Thomas Ullrich
10:30 AM	Combined discussion period for the preceding 4 talks	Discussion (20 min)
10:50 AM	Coffee Break	
11:15 AM	Community Input (EIC related)	
12:30 PM	Lunch Break	
1:30 PM	Discussion about EIC White Paper	
Reports		
2:45 PM	Report from the Computational Nuclear Physics Town Meeting 1	Peter Petreczky
3:00 PM	Report from the Computational Nuclear Physics Town Meeting 2	Martin Savage
3:15 PM	Report from Educational Town Meeting	Thia Keppel
3:30 PM	Combined discussion period for the preceding reports	Discussion (30 min)
4:00 PM	Coffee Break	

Figure 15: Agenda of the joint session (Saturday/Sunday)

Sunday, September 14, 2014		
	8:30 AM - 4:00 PM Joint Session	
	4:00 PM Coffee Break	
	"Phases of QCD" session on low x, p+A, and spin	
	4:30 PM -- Theory: Unique opportunities in p+A collisions at RHIC and LHC	Zhong-Bo Kang
		Discussion (10 min)
	5:00 PM -- p+A experiments at RHIC and the LHC and related upgrades	John Lajoie
		Discussion (10 min)
	5:30 PM -- Opportunities for RHIC Spin in the Coming Decade	Elke Aschenauer
		Discussion (10 min)
Monday, September 15, 2014		
Day 3: Phases of QCD Talks and Discussion	Jet Studies of QCD matter	
	8:30 AM -- Jets at RHIC & LHC: probing the QGP at multiple length scales (theory)	Xin-Nian Wang
		Discussion (10 min)
	9:00 AM -- Jet studies at LHC & RHIC now and tomorrow	Gunther Roland
		Discussion (10 min)
	9:30 AM -- "What jets studies at RHIC can tell us about QGP properties"	Jamie Nagle
		Discussion (10 min)
	10:00 AM Coffee Break	
	Heavy quarks and quarkonium as a probe of the QGP	
	10:30 AM -- Experimental summary of the next decade with Heavy Quarks and Quarkonium	Lijuan Ruan
		Discussion (10 min)
	11:00 AM -- Theory: what we know about the QGP from HQ and what we can still learn	Derek Teaney
		Discussion (10 min)
	Community Input & White Paper Discussion	
	11:30 AM -- Community input	
12:30 PM Lunch		
1:30 PM -- Community input		
2:30 PM Phases of QCD White Paper: discussion and polishing of draft	Town Hall Conveners	
	recommendations	Discussion
	3:30 PM Coffee Break	
	4:00 PM Vote on recommendations; structure of White Paper; writing assignments	
	5:30 PM Adjourn	

Figure 16: Agenda of the “Phases of QCD Matter” parallel session, part II (Sunday/Monday)